Research Article

Roberto Muscia*

Mechanical Design of Innovative Electromagnetic Linear Actuators for Marine Applications

https://doi.org/10.1515/eng-2017-0033
Received Jul 09, 2017; accepted Sep 08, 2017

Abstract: We describe an engineering solution to manufacture electromagnetic linear actuators for moving rudders and fin stabilizers of military ships[1]. The solution defines the transition from the conceptual design of the device initially studied from an electromagnetic point of view to mechanical configurations that really work. The structural problems that have been resolved with the proposed configuration are described. In order to validate the design choices discussed we illustrate some results of the numerical simulations performed by the structural finite elements method. These results quantitatively justify the suggested mechanical solution by evaluating stresses and deformations in a virtual prototype of the structure during its functioning. The parts of the device that have been studied are the most critical because in cases of excessive deformation/stress, they can irreparably compromise the actuator operation. These parts are the pole piece-base set and the retention cages of the permanent magnets. The FEM analysis has allowed us to identify the most stressed areas of the previous elements whose shape has been appropriately designed so as to reduce the maximum stresses and deformations. Moreover, the FEM analysis helped to find the most convenient solution to join the pole pieces to the respective bases. The good results obtained by the suggested engineering solution have been experimentally confirmed by tests on a small prototype actuator purposely manufactured. Finally, a qualitative analysis of the engineering problems that have to be considered to design electromagnetic linear actuators bigger than the one already manufactured is illustrated.

Keywords: linear actuator, conceptual design, mechanical design, FEM, solid modelling, structural analysis, stress, deformations, vibrations

1 Introduction

The rudder represents one of the main devices used to steer boats. In order to warrant the safety of the navigation, such device must always work correctly. Therefore, the reliability of the whole system of the rudder driving has to be very high, especially when the burden of the ship is high. In these ships, the forces required for driving a rudder can be equal to many tons and the system that rotates the same rudder is quite complex.

Two types of actuators, oleodynamic rotary and linear [1] are always used for the operation of large ship rudders. For decades only these two systems have been used and there has been no research or innovation that was intended to replace them with more efficient systems. However, the research has focused heavily on the control of the rudder and fin stabilizers in relation to the stability and vibrations [2–5]. In these studies, sophisticated mathematical physical models are presented, assuming certain trends of the forces generated by the actuators, but which do not represent the topic of the research. In this regard we can observe that at present, a common rudder driving system for high burden ships is based on the oil-pressure rotary actuators [1] (see Figure 1). In these motors, oil is pumped with high pressure and a very slow rotation of the motor pistons around an axis is generated. The pistons are jointed with a shaft that supplies a high torque and this shaft rotates the rudder by suitable operating levers. The magnitude of the rotation of these motors is limited and usually does not exceed 150 degrees. Over the years, the experience of the management of the whole system (pumps, valves, control systems, etc.) that allows the operation of the rotary actuator showed significant problems in relation to maintenance and regulation/control of this kind of devices. Therefore, in order to ensure the proper functioning of the rudder, checks, revisions and maintenance of all system components must be carried out regularly. The costs associated with these activities, the relatively high overall dimensions and weights of the system and also some technical difficulty in regulating the operation according to the needs of navigation have motivated the study of alternative devices to rotary actuator working by oil-pressure. A

1 Italian Ministry of Defence, General Direction of Naval Equipments (NAVARM), Projects ISO (2012-2014) and EDDA (2015-2017).

***Corresponding Author: Roberto Muscia:** University of Trieste, Department of Engineering and Architecture, Via A. Valerio n.10, 34127 Trieste, Italy; Email: muscia@units.it

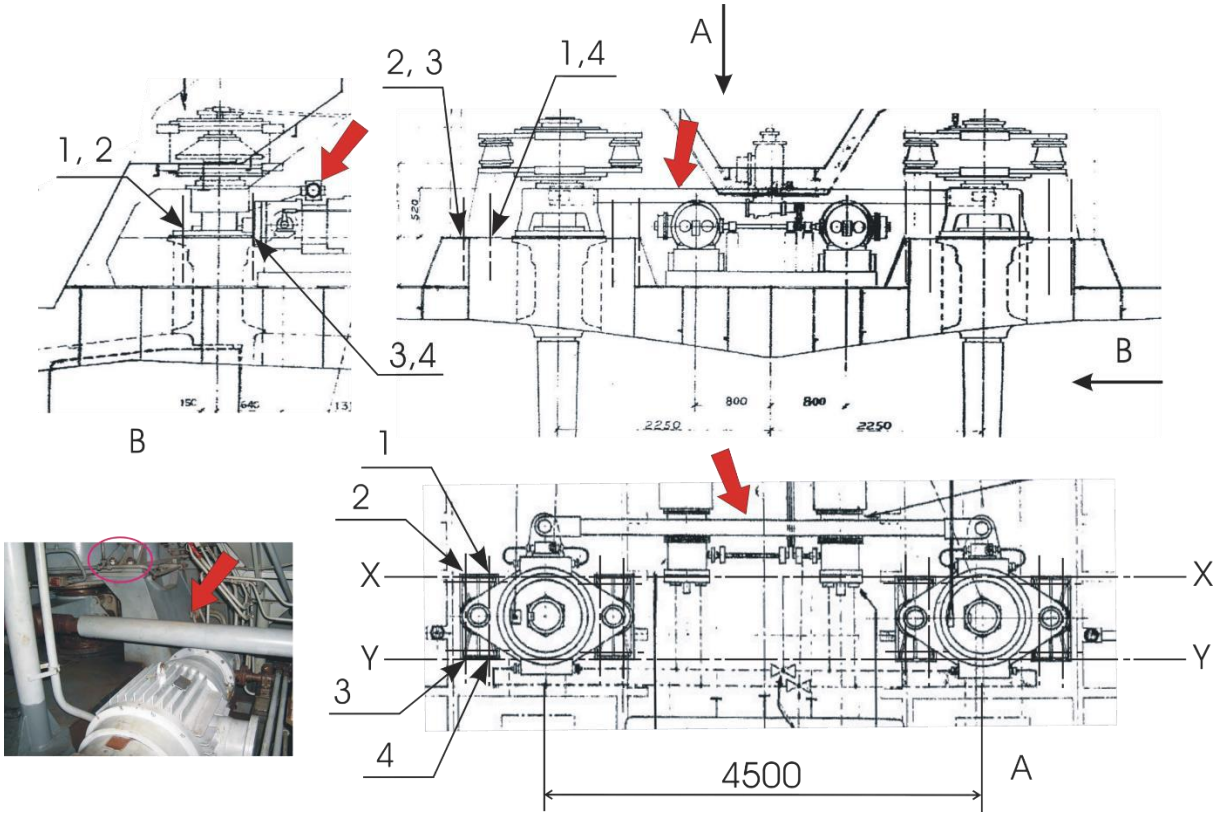

Figure 1: A twin rudder driving system of a military vessel based on oil-pressure rotary actuators (the red arrows indicate the rudder operating levers).

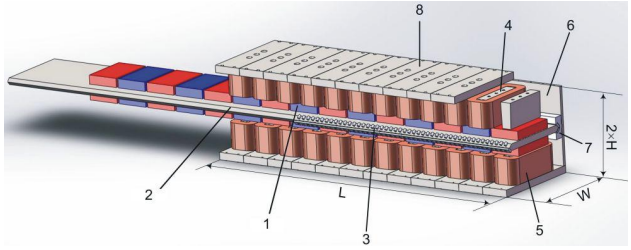

Figure 2: A conceptual configuration of the electromagnetic actuator proposed [6].

possible alternative that has been studied at a conceptual level is represented by innovative electromagnetic linear actuators able to develop some tons of thrust with limited strokes (1000-1200 mm) [6–13]. The novelty of this actuator involves the complete replacement of the oleodynamic system traditionally used with an electromagnetic device. Therefore, it is possible to manufacture a device for the rudders operation of the ships that will be much cleaner and adjustable than those using the pressurized oil that is pumped into the oleodynamic actuators. In this way the pressure and oil flow control system is no longer needed and the whole control of the system becomes electrical/ electronic with undoubted advantages of cleaning and precise adjustment possibilities.

Figure 2 illustrates the conceptual design of the electromagnetic device proposed. A set of permanent magnets (1) is placed in contact with the upper and lower surfaces of a steel plate (2) driven by suitable bearings. These bearings are integral with the frame of the device and allow the translation along the horizontal direction of the same plate (the so-called *mover*). The polar expansions (4) are positioned in correspondence with the magnets and the electrical windings (5) are arranged around these expansions. A gap of 3 mm is fixed between the magnets and the flat surfaces of these polar expansions. By powering the windings in a controlled way, it is possible to generate the magnetic forces that move the mover driven by the relative bearings. These forces can be extremely high. Therefore, the mover is able to apply a very strong push to a suitable lever mechanism which converts the rectilinear motion into a rotational motion. This mechanism consists of a prismatic rotary joint that rotates the rudder (see Figure 3). The rudder rotates along a clockwise or coun-

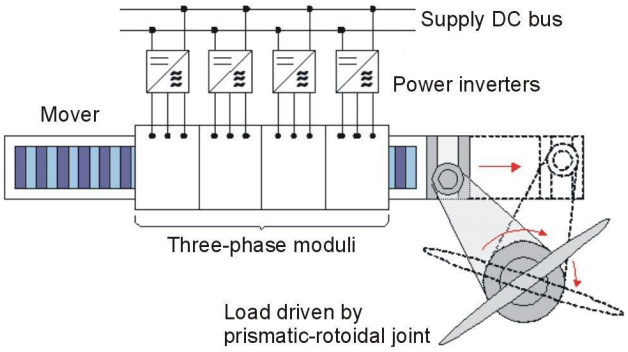

Figure 3: Transformation of the movement of translation into a rotation to drive the rudder [11].

terclockwise direction depending on the direction of motion of the mover. A suitable sizing of the kinematic system allows one to obtain the correct rotation angles. Accurate calculations [6–8] have identified the right sizing of the conceptual configuration of the actuator illustrated in Figure 2. These simulations initially involve the calculation of the horizontal electromagnetic thrust applied to the steel plate (2) (see Figure 2) that the device can develop. From these calculations [6–8], it results that the thrust generated by this suitably dimensioned actuator which can also be assembled in the stern of a ship, can reach or exceed that generated by traditional oleodynamic actuators. Based on these results, further studies [11, 13] were carried out to assess the practical possibility of replacing the oleodynamic actuators with the electromagnetic actuators for the operation of military ships rudders. These studies, based on numerical simulations, have been further elaborated with experimental tests and simulations. Detailed studies concerning the heating problems caused by i) eddy currents [9], ii) power supply, and iii) control via inverter of the electromagnetic device [10] have also been performed. Experimental tests were carried out by manufacturing an electromagnetic actuator prototype that can apply a horizontal thrust greater than 3 tons on the steel plate (2) (see Figure 2) [11]. Another problem that has been studied to develop this kind of actuator concerns the reliability of operation. In this respect, simulations and tests [12] were performed in relation to the possible malfunction of a single module consisting of the polar expansions (4), the electrical windings (5) and the base (8) (see Figure 2). This is to assure the decoupling between the stator modules, so that a possible short circuit occurring in a module does not affect the others and the device can still operate, though with reduced performance.

However, in order to manufacture a first working prototype of the device, it has been necessary to study carefully the whole system from a mechanical point of view. The mechanical structural solution described in the following paragraphs has been developed by studying design configurations characterized by sufficiently reduced stress/strain. In this way, the electromagnetic sizing previously defined has been met and the device operates properly.

2 Stiffness and Strain Problems of the Structure

One of the main problems considered to transform the conceptual design shown in Figure 2 into a working electromechanical device concerned the stiffness of the system. In order for the device to work properly, it is necessary that during the operation of the machine, the air gaps between the permanent magnets and pole pieces are kept as constant as possible. When the current circulates in the windings, very high tensile forces are applied to the pole pieces. These forces tend to lengthen the poles, reducing the air gap. At the same time, the magnetic force that forces the mover to translate, flexes the polar expansions. Therefore, these parts are generally subject to tensile and bending stresses. These actions have to be appropriately balanced by the reactions generated from the structure that support the same polar expansions. As illustrated in Figure 2, there are 12 polar expansions on a side of the mover and other 12 on the other one, hence, very strong forces will be generated. These forces tend to strain the frame on which the same pole pieces are fixed. In order to get a proper functioning of the actuator, these strains must be very small (0.01-0.1 mm), otherwise the air gap depending on operating conditions changes and control of the forces generated by the mover could become problematic. Another important aspect that has been considered to engineer the conceptual design shown in Figure 2 concerns the positioning of the magnets on the mover. These magnets, illustrated in Figure 2 by simple red and blue parallelepipeds, are actually constituted by small magnets parallelipeds side by side. In this way, sets of nine samarium cobalt magnets (grade YXG30, HcB 835 KA/m) placed side by side have been used to come near each “big” magnet (1) illustrated in the conceptual design (see Figure 2). These magnets, when external magnetic fields are null, adhere to the top and bottom surfaces of the mover, which is manufactured by using ferromagnetic steel. However, the horizontal magnetic forces that act during the operation of the machine can be higher than the friction forces in correspondence to the magnets-mover contact surfaces. It follows

that the friction does not warrant maintaining each magnet in the correct position established in the electromagnetic design of the system. Moreover, in case of a short circuit, high currents could demagnetize the magnets. This fact would cause a dangerous situation because the magnets could be attracted by the pole pieces. In this case, the gap would not exist resulting in the blocking of the mover and severe damage of the actuator. In relation to the reliability aspects, the probability of this occurrence must be extremely small. Therefore, the engineering solution has considered the design of cages retention (manufactured in non-magnetic aluminum alloy) for the magnets so as to keep them always in contact, in the right position, with the mover surfaces to which they normally adhere. These cages of retention (see Figure 4) have been arranged facing the two sides of the mover. The joint between each pair of opposite retention cages was performed by simple and reliable bolts (the mover has through holes in correspondence to the stems of the screws). The electromagnetic calculation has provided the maximum value of the force to which the permanent magnets would be subject in the case of demagnetization. By using this value of force, accurate structural FEM analyses have been performed to evaluate stress and deformation of the retention cages if the previously described malfunction occurs. The fitness of these simulations was checked by plotting suitable curves of convergence relative to the equivalent tensile stresses (in accordance with Von Mises criterion) found in the most stressed regions. These cages have been also sized to resist against the force applied along the horizontal direction that the magnets themselves generate to obtain the regular translation of the mover. Therefore, if the magnets lose the adhesion resulting from the frictional force between the surface of the mover and that of each magnet in contact with the mover itself, the cages prevent any slipping. Finally, another important aspect to transform the conceptual design illustrated in Figure 2 into a working mechanical system involves the coupling between the mover and the frame. The mover must be able to move with very little friction relatively to the frame on which all the polar expansions are fixed. A feasible solution has been found by replacing the conceptual coupling based on cylindrical rollers (see the guide (2) and the rollers (3) in Figure 2) by six recirculating ball bearings fixed to the machine frame. These bearings allow the translation of the straight guides connected by screws to the longer sides of the mover. In this way, a good sliding motion of the mover across the frame has been obtained, even when the same mover abundantly came out of the machine body. Referring to the mover-bearing-frame coupling, the solution adopted shows a certain degree of hyperstaticity. In general, it would always be appropriate to consider constraining of isostatic type, but in relation to the high loads applied to the mover (which can also be subject to lateral instability) we have preferred the hyperstatic solution. However, we observe that it was possible to adopt this solution because the lengths of the frame and the mover in the case study are not too high (the frame is approximately 1000 mm long and 500 mm wide, the length of the mover does not exceed 2000 mm). Consequently, all the flatness, parallelism, etc. errors that affect the frame on which the six bearings have been assembled are limited.

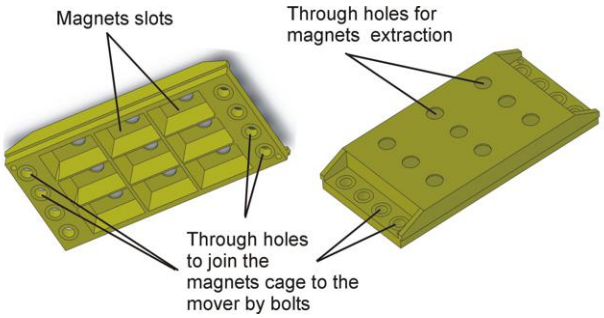

Figure 4: Retention cages of the magnets.

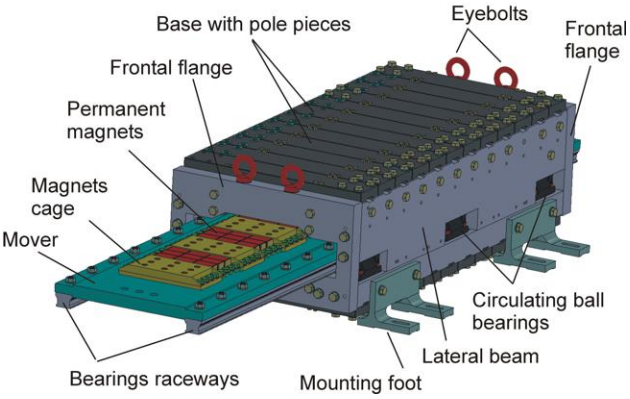

Figure 5: Solid modelling of the electromagnetic actuator.

3 Architecture of the Mechanical Solution

The mechanical solution studied to make the device shown in Figure 2 functional has been illustrated in Figure 5. Through examination of this figure we note that all the pole pieces (4) and the relative base (8) (see Figure 2) are fixed on an aluminum alloy frame with front flanges. These flanges have an opening that allows the mover to come out from the two sides of the structure. Figure 6 illustrates the coupling between the mover and the frame by

recirculating ball bearings. This figure also shows the position of the magnet cages and the coils inserted around the ferromagnetic cores (pole pieces). The configuration of these ferromagnetic cores has been the subject of an especially accurate investigation because the clamping of the same cores to the relative bases must be very reliable. In this regard, various solutions have been considered. Figure 7(a) shows the pole piece-base joined by fourteen screws. In this case the lower end of the pole piece shows two jutting side edges with through holes where the fourteen screws are inserted. Another kind of joint illustrating a dovetail coupling is shown in Figure 7(b). In the center of the guide a parallel pin is inserted which eliminates the translation degree of freedom of the pole piece with respect to the guide. Otherwise, Figure 7(c) illustrates the insertion of three parallel pins instead of only one. In this case the diameter of these pins is lower than that of the pin shown in Figure 7(b). Another solution (see Figure 7(d)) excludes the use of pins. In order to lock the pole piece in the right position, the solution in Figure 7(d) considers the insertion of two shaped elements in the groove of the dovetail joint. These two parts are fixed onto the base by cap screws. In Figure 7(c) the two hangers that lock the induction coil around the polar expansion are also illustrated in the correct position (see also Figure 6). Finally, the last solution has considered the manufacturing of the polar expansions and bases enbloc. Figure 8 illustrates the technical drawing of this part. This latter solution is the one that has been adopted. As a matter of fact, the results of numerical simulations relative to deformations and stresses of the complex base-polar expansion suggested that this latter solution was acceptable. At the same time, in relation to the cost and precision, it is very advantageous to manufacture the complex base-expansion enbloc. Therefore, it was decided to adopt this solution. It was observed that in electric motors, polar expansions are usually manufactured by using silicon-iron laminations. This solution limits the effect of the eddy currents that result in the heating of the part and decrease the system efficiency. The intensity of these currents depends on the frequency of the winding power supply (the higher the frequency, the greater the heating). However, in the case study of the linear actuator, the use of a polar expansion consisting of a single piece of steel is not a problem because the current frequency with which the single winding is powered is very low (lower than 1 Hz), therefore the heat generated is moderate [9].

The manufacturing of the part enbloc has been performed by starting from a steel bar with rectangular section. From this parallelepiped of steel, by using oxygen cutting and a suitable machining allowance, each base-pole piece was obtained. Subsequently, by applying an

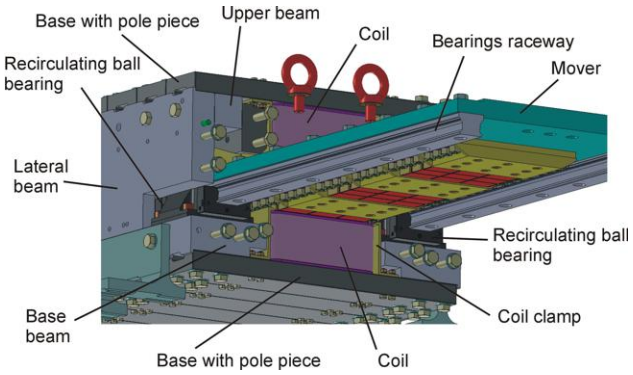

Figure 6: Internal structure of the electromagnetic actuator.

annealing procedure, deformations and residual stresses caused from the rapid cooling from the oxygen cutting temperature to the room temperature were reduced. By this heat treatment, the surface layer of martensite that is spontaneously formed because of the previously mentioned cooling was eliminated. After the transformation of the martensite in pearlitic/ledeburitic structures, much less hard and brittle than the martensite, chip-forming machining processes have been carried out. In this way, the precise dimensions of the part were obtained. It was observed that a chip-forming machining of the part before the annealing could cause the breaking of the cutting tool (the martensite is very hard and not workable). Even though technically feasible, from the cost and assembling point of view, the other solutions studied are less convenient. The possibility to weld the pole piece on the base has been also considered. However, this solution was discarded because of the cost, the residual stresses and deformations related to the difficulty to obtain a good weld with high penetration. With reference to the recirculating ball bearings for the translation of the mover, in Figure 9 a possible alternative arrangement to that adopted (see Figure 6) is illustrated. In this case the guides of the bearings are fixed on the longer sides of the mover. However, this solution even if feasible, was discarded because i) it is necessary to manufacture a high number of hangers to correctly place and lock the bearings, ii) the mass of the mover, iii) the number of screws to fix the guides, and iv) the width of the mover significantly increased. It was also observed that a wider mover causes an increase of the width of the whole actuator (the increase is about equal to 120 mm with respect to the 490 mm of width relative to the solution shown in Figures 5 and 6). Consequently, by choosing this arrangement of the guides, it would have been necessary to increase the length of the bases on which the polar expansions are fixed. Therefore, this choice causes an increase of stress and deflection of the complex base-polar expansion

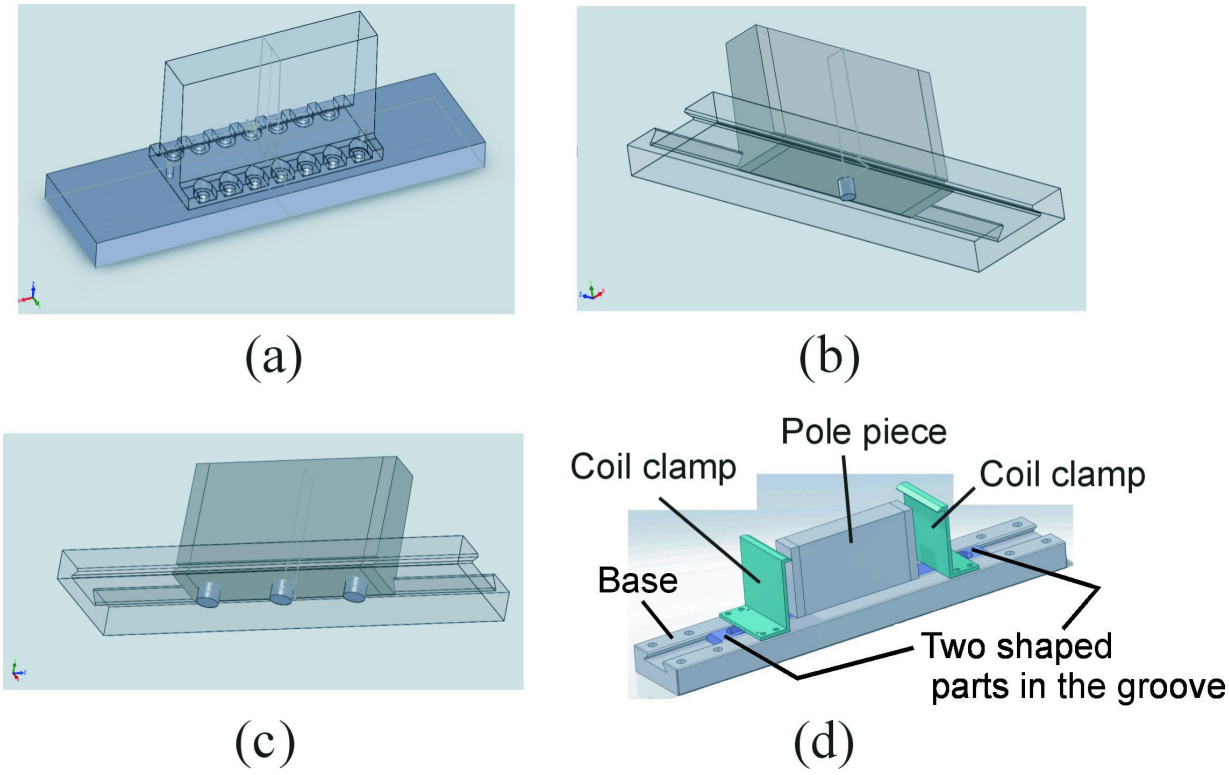

Figure 7: Clamping solutions of the ferromagnetic core to the base by (a) screws, (b) a dovetail coupling with one parallel pin, (c) three parallel pins, and (d) insertion of two shaped elements in the groove of the dovetail joint.

when the electromagnetic forces are applied. As a matter of fact, these forces are very intense and tend to bring the expansions toward the upper surface of the magnet cages by reducing the air gap. Figure 10 shows the final technical drawing of the manufactured actuator frame. The dimensions of the frame are equal to 1104 × 490 × 266 mm and the bases of the pole pieces (see Figure 8) have a thickness equal to 30 mm. As a result, the total height of the actuator is 266 + 30 + 30 = 326 mm. The mover has a length and thickness of 30 and 1845 mm, respectively, and the width is equal to 404 mm.

4 Structural Mechanical Simulation of the Prototype

The particular solutions adopted to obtain the correct functioning of the electromagnetic actuator manufactured have been found by studying the mechanical strength of the system when it generates the maximum thrust. Therefore, the mechanical design has been developed with reference to the following elements: i) starting from the conceptual design of the device, all the sizes that need to be met to obtain the proper functioning of the electromagnetic system are known, ii) the maximum electromagnetic forces generated by the device and the external reaction forces are known, iii) the admissible maximum reduction of the air gap between the pole pieces and the facing surface of the cages of the permanent magnets mounted on the mover is known, iv) it is considered a serious situation of malfunctioning of the device (a short circuit, overload, etc.) that induces the demagnetization of the magnets retained by the cages, v) as a consequence of the demagnetization we suppose that the magnets behave as a normal ferromagnetic material subject to the action of attraction of the pole pieces, vi) in relation to the previous hypothesis of malfunction, a structural analysis of each cage retention is performed (the cages must be able to retain the magnets in the correct position even when there is no more magnetic attraction between the mover and the magnets themselves), vii) in this case we considered two components applied to the retention cage: one tends to cut the cage off the mover along the direction perpendicular to the surface of the mover on which the cage is fixed and another has a direction parallel to the translation axis of the same mover. The load hypothesis defined by the above-mentioned malfunction is justified because if the magnets behave as simple ferromagnetic materials, owing to the action of the magnetic pole pieces, they tend to slide very

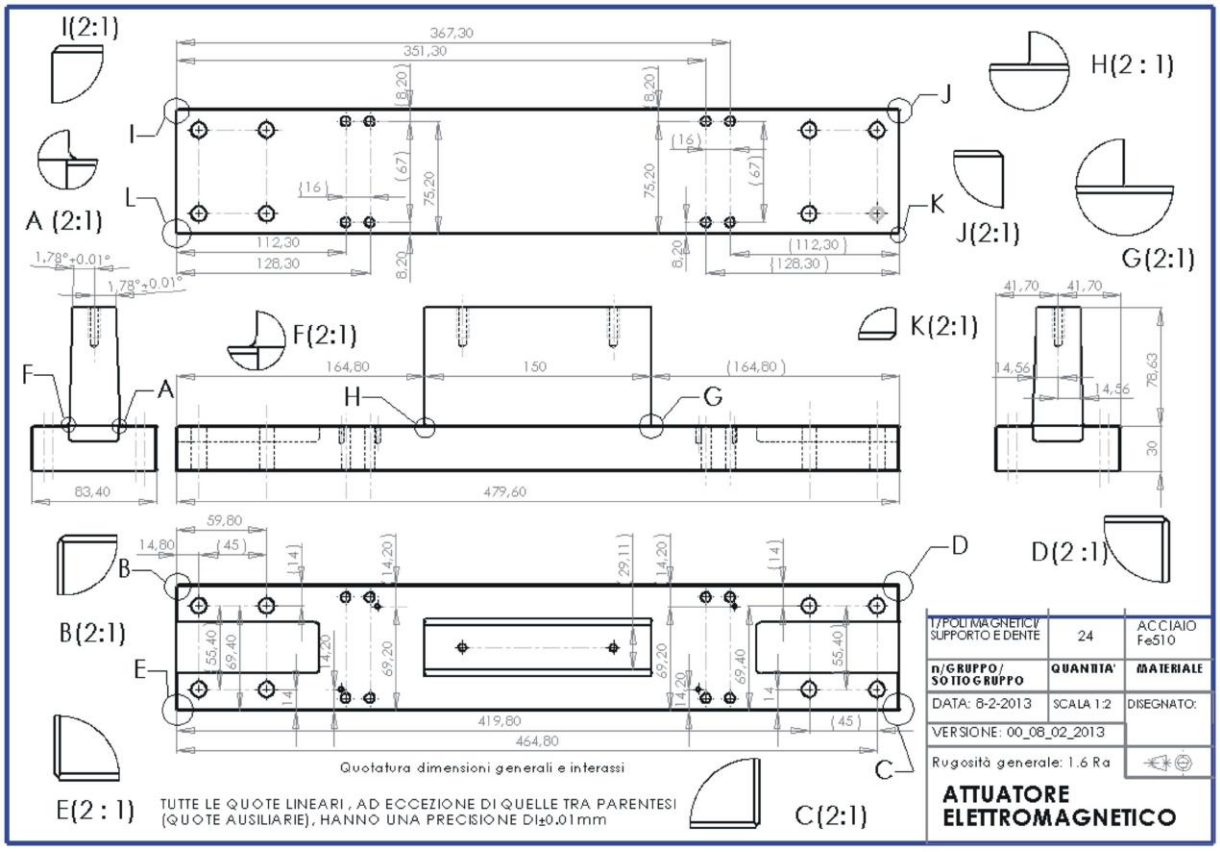

Figure 8: Ferromagnetic core and base enbloc.

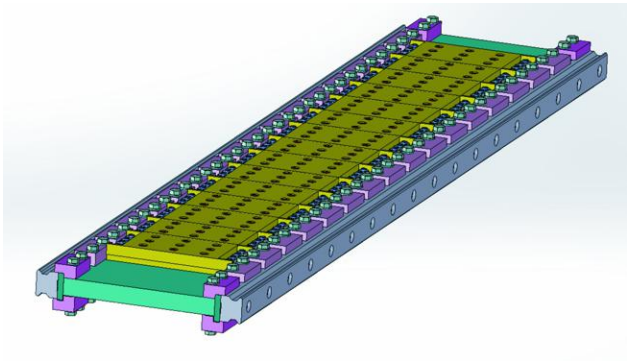

Figure 9: Alternative arrangement of the recirculating ball bearings for the translation of the mover.

easily on the surface of the mover and the only obstacles to this displacement are the side contact surfaces of the housings magnets within the cages. The stresses that could be applied to the prototype by the mounting feet if the base to which the actuator is fixed is deformed were not taken into account. As a matter of fact, the actuator manufactured represents a laboratory prototype which is currently primarily intended to validate experimentally the performance provided by numerical simulations. Therefore, the device will not be put in any hull that could deform and stress the structure of the device through any significant displacements imposed on the mounting foots. The final part of the paper illustrates the problems that need to be studied to design more powerful actuators to actually install into a hull.

In relation to the complex shapes of these parts, a structural study based on nominal strength models can be very difficult. Stresses concentration caused by changes of shape, grooves, etc. are computable with precision only when the relative concentration factors are known. In the case study, these factors are not known thereby making a structural analysis based on the Finite Element Method (FEM) is suitable. The FEM structural simulation of the above-mentioned cages has been performed by applying magnetic forces on the surfaces of the magnets housings. Actually, these forces are applied to the demagnetized magnets that, without the cages, should be shifted horizontally and vertically with respect to the surface of the mover. With reference to the criteria outlined above, the load conditions to perform the structural analysis of the actuator have been defined. The following paragraphs describes the finite element simulations and the results ob-

Table 1: Material Used to Manufacture the Actuator.

	Base-Polar Expansion Steel *EN 10025-2: 2004*	**Magnet Box Aluminium Alloy** *UNI 9007/2*	**Frame Alloy Aluminium** *EN AW-6101*
Conventional Designation IT	Fe510C – S355JO	P-AlZn5.8MgCu	P-AlSi0.5Mg
Numerical Designation	1.0553	7075	6101
Alphanumeric Designation B.S.	50C	2L95/L160	TE
Ultimate tensile stress	470-630 N/mm^2	520-647 N/mm^2	294-343 N/mm^2
Yield tensile stress	355 N/mm^2	481-589 N/mm^2	265-304 N/mm^2
Percentage elongation	22%	5-10%	5-9%

tained relatively to the most critical parts of the actuator, *i.e.* the base-pole piece set and the magnet cages. Additional finite element analysis was performed on the actuator frame on which the above elements are assembled. These analyses have furnished extremely small deformations and stresses. In Table 1 the materials, with their characteristics, that have been used to manufacture the various parts of the actuator are reported.

5 Structural Analysis of the Polar Expansions and the Base

Three possible choices have been considered to manufacture the base-polar expansion set: i) separate polar expansion and joined to the base by screws (see Figure 7(a)), ii) separate polar expansion and connected to the base by a dovetail coupling (see Figures 7(b)-7(d)), and iii) polar expansion and base enbloc (see Figure 8). For each of these choices the heaviest load condition shown in Figure 11 has been considered. The forces indicated in this figure represent the electromagnetic forces calculated by the simulations previously performed [6–8]. These forces have been precautionarily applied only to the end edge of the pole, corresponding to the relative upper surface of the same expansion (see Figure 11). Actually, the magnetic forces act on the whole body of the polar expansion, with a certain distribution. Therefore, the moment calculated in accordance with the schematic representation shown in Figure 11 that tends to bend the same polar expansion, is significantly greater than that which actually acts. This load hypothesis has been considered both for simplicity and precautionary reasons. In the following paragraphs we describe the FEM analyses performed with reference to the three kinds of base-pole piece joints previously mentioned.

5.1 Polar Expansions and Bases Joined by Screws

The joint is shown in Figure 7(a). The FEM analysis of the system has been carried out by constraining the base to the end faces (see Figure 12). In comparison with the real restrain (eight screws, see Figure 5), this kind of constraint allows a greater pliability of the base. As a matter of fact, torsion on a greater length is allowed at the base. Concerning this issue, it was also observed that the part of the actuator frame where the bases are fixed with the eight screws is particularly solid and resistant and therefore is subjected to very little deformations. Consequently, the FEM schematization of the base constrained as a beam with both ends fixed allows a greater torsion and bending of the same base with respect to the device really manufactured. Therefore, concerning the displacements, the FEM analysis performed can be considered precautionary. The maximum displacements calculated along the axes Y and Z of the absolute reference system shown in Figure 11 are defined at the upper end of the pole piece. With reference to the forces applied whose values have been reported in Table 2, maximum displacements greater than

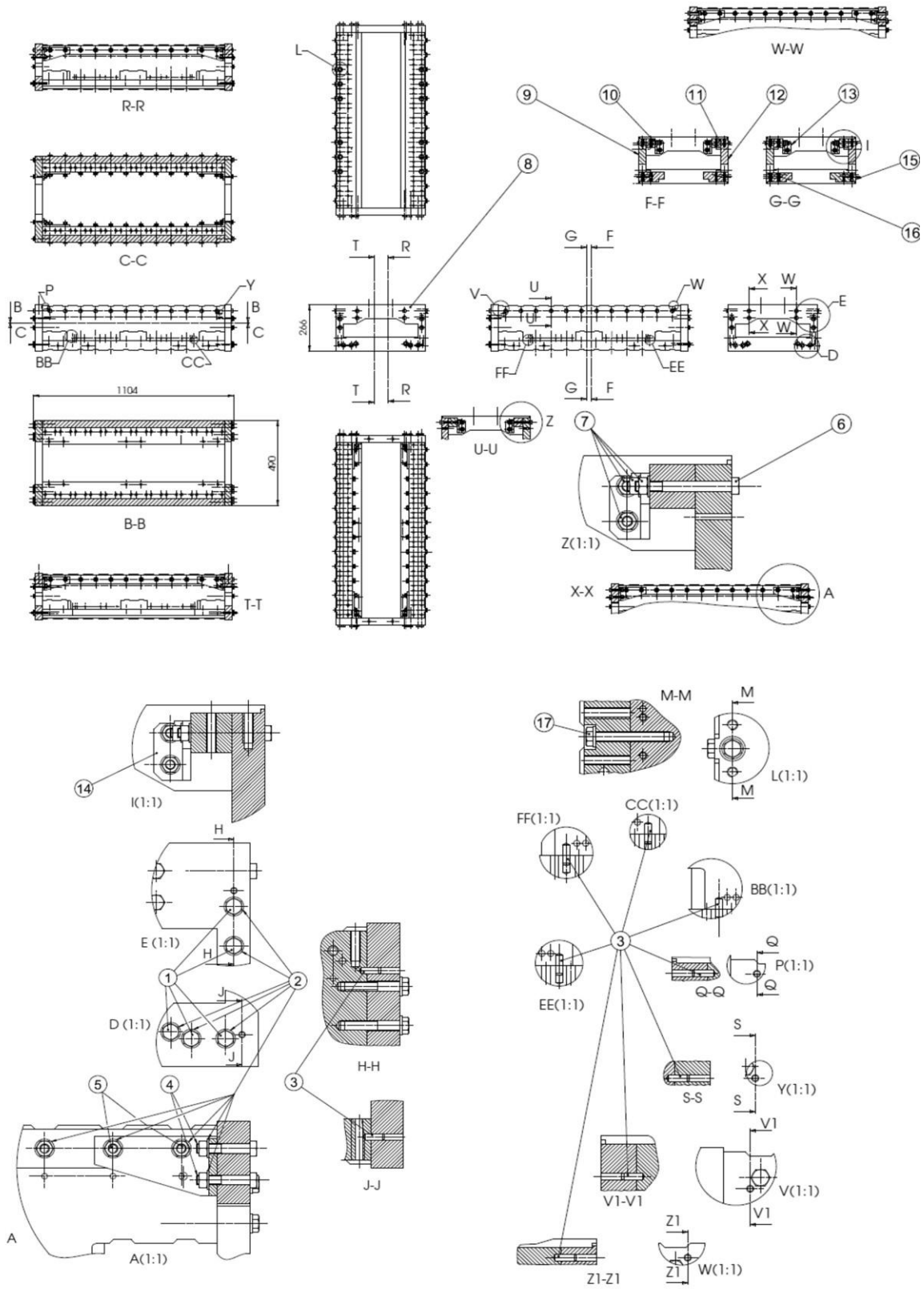

Figure 10: Technical drawing of the actuator frame manufactured in non-magnetic aluminum alloy.

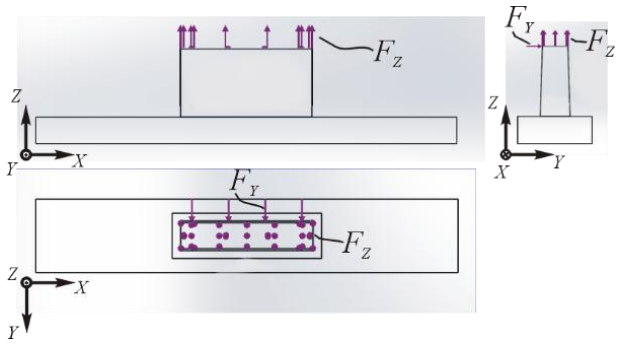

Figure 11: Forces applied to the polar expansions to perform the FEM simulations.

Table 2: Forces Applied to the Polar Expansions.

F_X	0 N
F_Y	3000 N
F_Z	7600 N

Table 3: Maximum Displacements of the System Base-Polar Expansions Joined by Screws.

U_X	0.00267 mm
U_Y	0.04 mm
U_Z	0.0157 mm

0.04 mm were not obtained. The direction and modulus of the forces indicated in Table 2 have been obtained from electromagnetic calculations performed in [6] with reference to the particular mechanical dimensioning of the device illustrated in Figures 8 and 10. These calculations are based on the models discussed in [6–8]. Table 3 reports the above-mentioned displacements towards the three directions *X*, *Y*, and *Z* (see Figure 11).

In relation to the proper functioning of the device, it was noticed that these displacements are more than acceptable, especially for the fact that they have been computed by using constraints which allow a greater torsion and bending with respect to the real configuration. With regard to the stresses, the maximum Von Mises stress σ_{id} has been evaluated according to a FEM linear model in the area ends bored and arranged to insert one of the fourteen joint screws. Moreover, in the case of demagnetizing of a single group of magnets housed in the corresponding cage, we note that the F_z component would not be more balanced by an equal and opposite force applied on the opposite side of the mover (it is assumed that a demagnetized magnet is like a ferromagnetic material). In this case, 7600 N would stress the recirculating ball bearings (see Figure 5) along the direction z (see Figure 11). This force is much weaker than the dynamic and static load factors C = 59200 N and C_0 = 91000 N, respectively, of the bearings adopted. Consequently, even in this critical situation, the normal operation of the bearings is assured. With reference to the material used to manufacture the pole piece (see Table 1), the value of the previous σ_{id}, equal about to 256 N/mm^2, is considerably lower than the yield strength of the steel used (see Table 1). It was also noticed that these results have been carried out by FEM simulations performed by using different mesh density in the areas of interest characterized by a fillet radius equal to 0.5 mm. Figures 12 and 13 show the point where the stress is maximum (see the red arrow). In this regard, for example, Figure 14 shows the convergence curve relative to the identification of the previously mentioned maximum stress σ_{id} in the point indicated by the arrow in Figure 13. The convergence curves of the FEM analysis have been defined by plotting the parameter of interest (stresses, displacements, etc.) versus a further parameter that represents the mesh density. This parameter can be the total number of finite elements used in the analysis, the number of nodes (n_{nod}), and the value of a local control of mesh density, etc.. In any case, when the parameter plotted (along the ordinate axis) during the mesh increase in the area of interest tends to be constant (for example the values oscillations are lower than 15-20% with respect the mean value in the last part of the convergence curve), we can be reasonably sure that this value represents the stress/displacement in the same area. Sometimes the parameter plotted very much increases its value versus mesh density (theoretically tends to infinity). In this case, the stress can be a *singular stress* [15, 16], which has to be correctly interpreted. Therefore, in order that the FEM analysis may provide reasonably correct results it is necessary to understand whether the stresses calculated are singular or not. The curves of convergence help to assess the reliability of the FEM results. Concerning the case study, all results were checked by plotting these curves and the presence of unusual stresses (in the areas of interest) has not been observed. The same check procedure has been applied to evaluate if the stresses computed were *spurious stresses* [17], another type of stress that can be generated in the FEM analysis in relation to numerical problems that has no bearing on reality. In the convergence curve shown in Figure 14, the point denoted by the letter A probably indicates a spurious stress value that must not be considered. The simulation of the joint base-pole piece has been performed i) fixing a coefficient of friction between the contact surfaces of the two parts and ii) applying to the surfaces defined by the contacts base-washer and pole piece-under

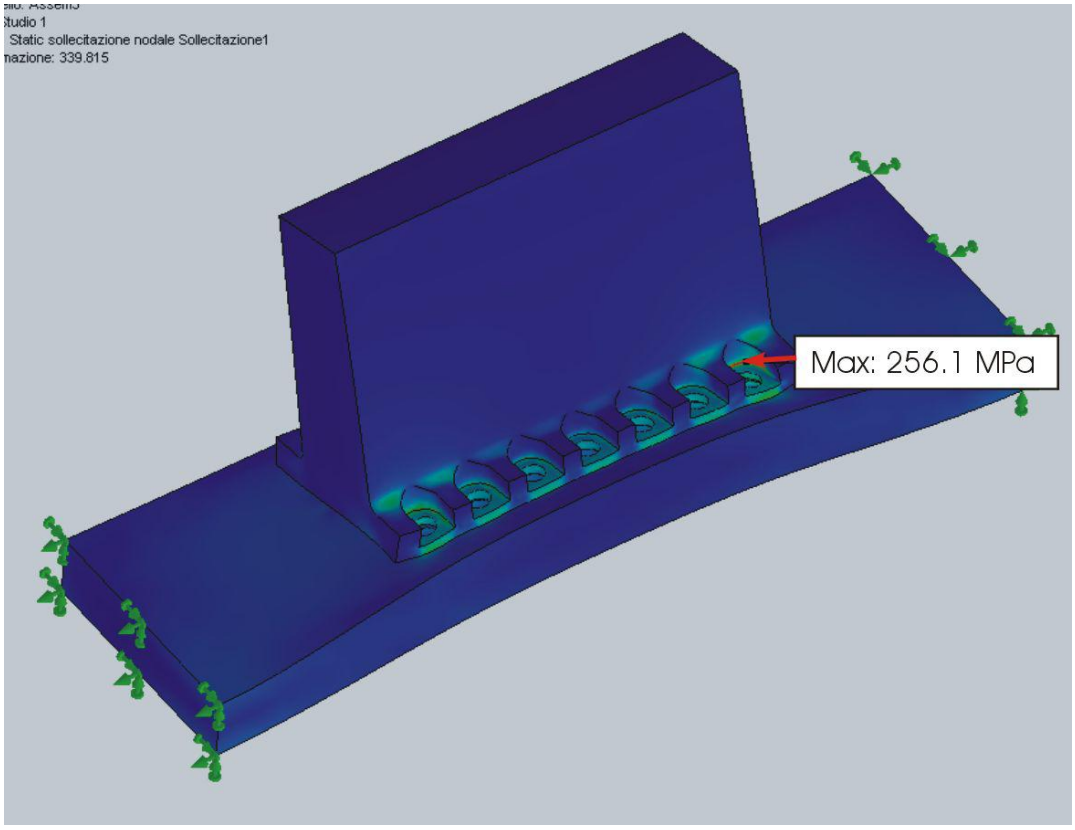

Figure 12: Maximum stresses and deformations evaluated by FEM analysis of the base - pole piece set joined by screws.

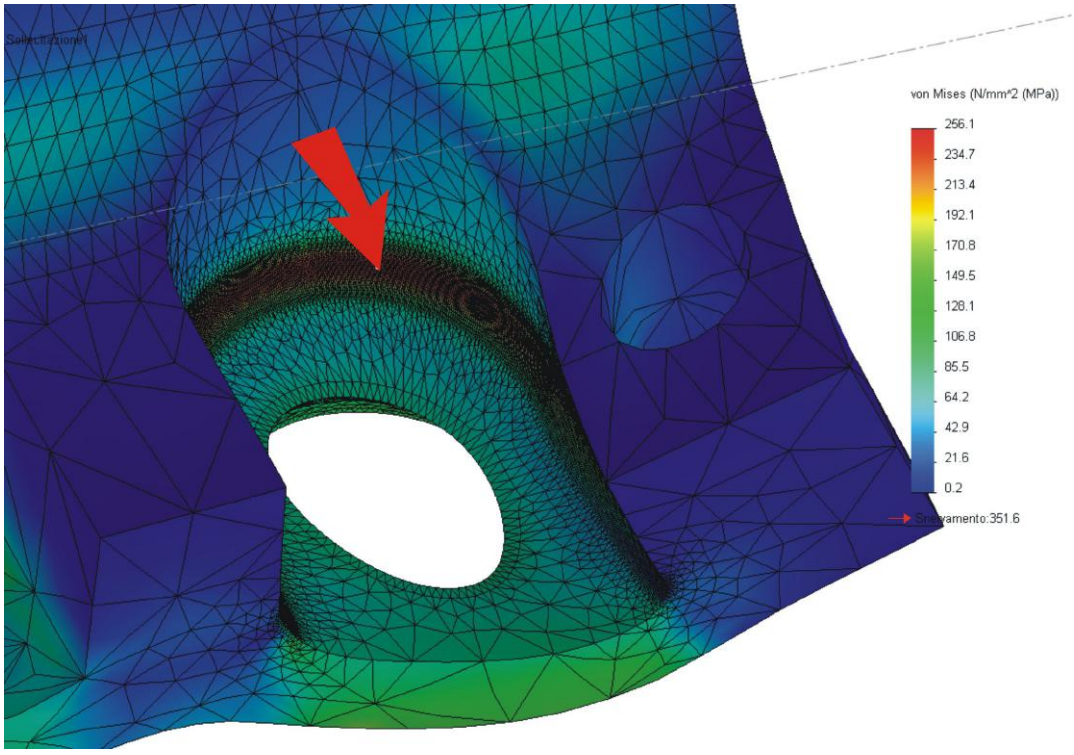

Figure 13: Areas of the base-pole piece set joined by screws where the stress is maximum.

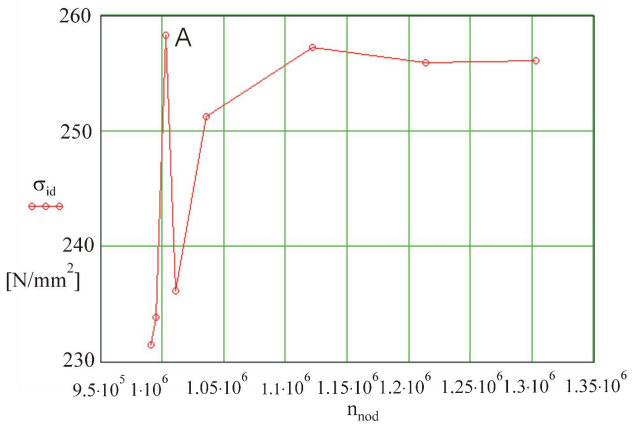

Figure 14: Convergence curve to check the stress σ_{id} in the highly stressed area indicated in Figure 13.

head of the screw-base the clamping force generated by the bolts. The screws, nuts and washers were not modeled, but the forces generated by these bodies have been applied to the FEM model on the surfaces previously defined. The clamping force generated by each screw was fixed equal to 10000 N. In this way it was possible to analyze the state of stress/deformation of the system by a numerically fairly light finite element model constituted by only two parts. As a matter of fact, the model is characterized by only one contact that is between the lower surface of the pole piece and the upper surface of the base.

5.2 Polar Expansions and Bases Joined by Dovetail Guide

The joint is illustrated in Figures 7(b-d). FEM simulations have been performed for all the three kinds of solutions indicated in the figures. Values of force equal and lower than those shown in Table 2 were used for the FEM computations. The results obtained with the insertion of the parallel pins (see Figures 7(b,c)) have provided very high stresses in correspondence to the insertion holes of the same pins. This solution, designed to obtain a firm positioning of the pole piece within the groove, has not even reduced the displacements with respect to those relative to the joint obtained by screws. On the contrary, the solution without pins indicated in Figure 7(d) has provided acceptable results. Figure 15 shows an example of FEM simulations concerning this kind of joint. The characteristic deformation of the system and the stress concentration at the end of the coupling was noticed. This area is well highlighted in Figure 16. A high mesh density was used to properly evaluate the stress in correspondence to a fillet equal

Table 4: Maximum Displacements of the Polar Expansions and Bases Enbloc.

U_X	0.059 mm
U_Y	0.075 mm
U_Z	0.0087 mm

to 1 mm. The maximum Von Mises stress σ_{id} computed by a linear FEM model is equal to about 270 N/mm^2 (see the red arrow in Figure 16). In Figure 17 the relative convergence curve σ_{id}- n_{nod} with the indication of a spurious stress (see point A) is reported.

5.3 Polar Expansions and Bases Enbloc

In this case the pole piece and the base have been modeled as a single part. The technical drawing in Figure 8 shows the shape and dimensions of the part. Figure 18 illustrates instead the deformed shape of the system owing to the application of forces shown in Figure 11. The maximum displacements obtained are reported in Table 4. It is observed that for this piece enbloc, two sets of FEM simulations with two different values of radius of curvature relative to the edges of the pole piece (see Figure 19 and enlarged details A, F, G and H in the drawing shown in Figure 8) were performed. The two values of the radius caused significant differences between the two corresponding maximum ideal stresses evaluated according to Von Mises criterion. With the radius equal to 0.5 mm, the maximum ideal sigma is approximately equal to 340 N/mm^2, while with the radius equal to 1 mm, such stress is reduced to about 228 N/mm^2. In relation to the yield strength of the steel used (355 N/mm^2, see Table 1), it follows that the choice of the radius of 1 mm is definitely more appropriate. This stress is localized in the area where the three edges of the pole piece (see Figure 19) intersect. In Figures 20 and 21 two examples of convergence curves are reported. These curves show the values of the two maximum ideal stresses σ_{id} previously mentioned versus the total number of nodes n_{nod} of the FEM model.

6 Structural Analysis of the Boxes Restraining the Magnets

The stress in each retention cage of the magnets shown in Figure 4 has been calculated by considering two systems of external forces. Figure 22 illustrates the first sys-

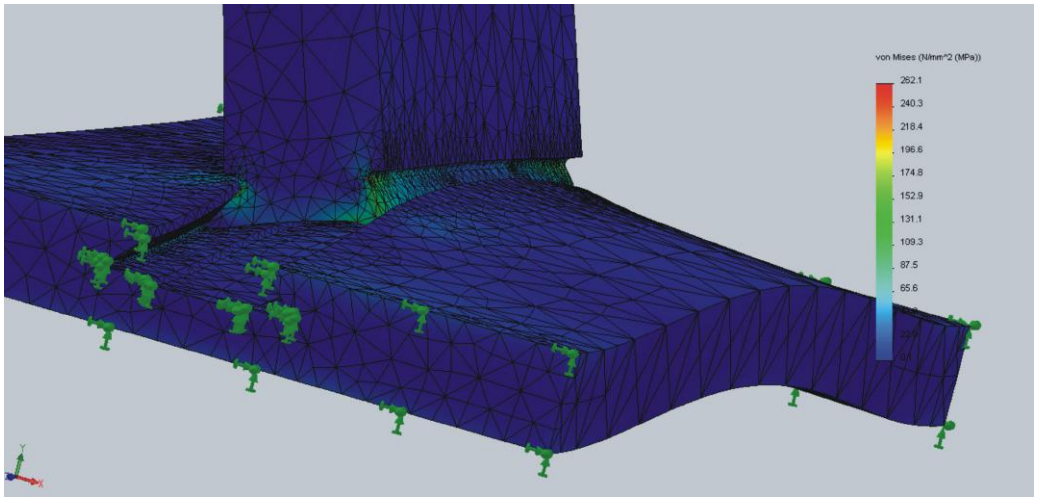

Figure 15: FEM analysis of the base - pole piece joined by a dovetail coupling.

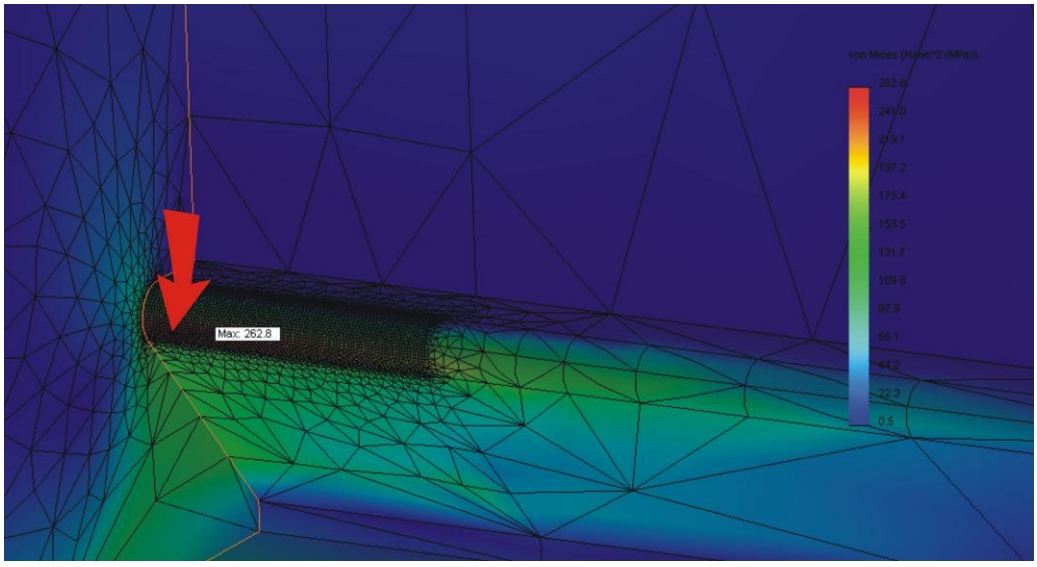

Figure 16: Stresses concentration in the dovetail coupling.

tem of forces. In this case the forces are applied perpendicularly to the nine bottom surfaces of each retention cage. These forces simulate a possible magnetic attraction of the pole pieces to each magnet in the unfortunate case where these magnets lose their magnetic characteristics and exhibit a ferromagnetic behavior (for example because of overcurrent owing to a short circuit). In this eventuality, the magnets must be held in place by the retaining cage which is consequently much stressed. In the simulations performed, the total force applied to the nine surfaces was assumed equal to 7600 N. The clamping of the cage on the mover by eight screws has been schematized by constraining both upper and lower circular crown contact surfaces where the washers apply the clamping load. This constraining has been simplified by fixed joints. In Figure 23 an example of FEM analysis of the cage is reported. The maximum displacement computed is of the order of tenths of millimeters. Concerning the stress, the maximum Von Mises stress σ_{id} has been observed in correspondence to the edge filleted with a radius of 2 mm (see the red arrow in Figures 22 and 24). Figure 25 shows the convergence curve $\sigma_{\mathrm{id}}(\mathrm{n}_{nod})$ that has allowed the identification of the above-mentioned stress whose value is slightly lower than 140 N/mm^2. In the convergence graph, the point A denotes almost certainly a spurious stress that, in this case, practically coincides with the pseudo asymptotic value shown in the same graph, *i.e.* with the maximum ideal stress that should affect the fillet. Finally, Figure 26 illustrates an example of the FEM analysis carried out by applying to the cage the forces indicated in Figure 22 simultaneously and

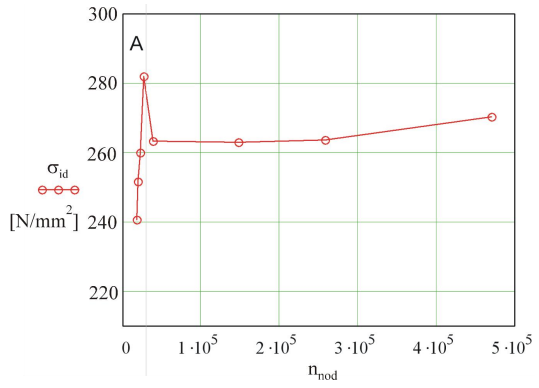

Figure 17: Convergence curve to check the stress σ_{id} in the fillet illustrated in Figure 16.

further 3000 N on the side surfaces of the housings of the same cage (see the arrows indicated in Figure 26). This simulation has been performed in order to verify if the cage is able to retain the magnets in the operating position when the same magnets lose their magnetization and become ferromagnetic. In this case, the magnets would tend to be dragged on the surface of the mover owing to the magnetic forces generated by the polar expansions. Considering the two systems of forces applied simultaneously, an ideal stresses σ_{id} about equal to 240 N/mm^2 has been obtained. This stress again affects the rounded edge shown in Figures 22 and 24 and its value is almost equal to two times the stress caused by the only one force system shown in Figure 22. However, in relation to the yield strength of the aluminum alloy used to manufacture the cages (see Table 1), the previous 240 N/mm^2 can be considered acceptable.

7 Choice of the Final Design of the Prototype

The choice among the kinds of base-pole piece joints previously described has been made according to the results obtained by the FEM simulations and the easiness of manufacturing (especially in relation to the manufacturing cost). From the structural strength and deformation point of view, all the choices can be judged sufficiently reliable (at least with reference to making of a first actuator prototype). Consequently, according to the cheapness criterion, it was decided to manufacture the system base-polar expansion enbloc (for example, see Figures 8). With regard to the retention cages, in relation to the high strength aluminum alloy that has been chosen to manufacture them (see Table 1), the FEM analyses indicate that stresses and deformations are acceptable, even if the permanent magnets lose their magnetization. In accordance with the results of the structural analyses performed, the actuator has been manufactured and tested. The performances obtained were similar to those computed by the electromagnetic computations [12]. The experimental tests show that the maximum thrust provided by the actuator and measured by a force sensor applied to the mover is almost equal to 32500 N [11]. The 3D modeling and FEM simulations have been carried out by using the SolidWorks and Simulation softwares [18], respectively. Figure 27 shows some photos of the linear electromagnetic actuator manufactured in the laboratory of Electrical Engineering of the Department of Engineering and Architecture at the University of Trieste.

8 Mechanical Problems of Bigger Electromagnetic Linear Actuators

The manufacturing and testing of the actuator prototype described in the previous sections have confirmed the possibility of manufacturing actuators of greater dimensions able to develop a thrust higher than 3 ton. However, the mechanical design of more powerful actuators implies solving important problems that do not affect the smaller actuators similar to that already manufactured and tested. As a matter of fact, in relation to i) the greater sizing of the system, ii) the installation, and iii) the environment where these high-powered actuators will have to work (stern zones near the engine room), it is necessary to consider other aspects concerning the sizing and forces that stress these devices. In this regard it was observed that the high-powered actuators to install on board of ships for driving the rudders, must be able to develop at least a thrust equal to 30 ton, *i.e.* ten times the thrust obtained by the prototype already manufactured. In order to achieve such result, it is necessary to size the system because the dimensions, the number of the polar expansions, etc. are increased. These modifications can cause the structural rigidity of the system to decrease. If such reduction is excessive, when the maximum thrust is developed, notable deformations of the device with consequent malfunctioning can occur. Moreover, large dimensions imply higher difficulty in satisfying the dimensional tolerances and most of all the geometric tolerances relative to the coupled parts. Consequently, in order to avoid forcing and/or wedging in the guides that support the mover of the actuator, it is necessary to pay particular attention when defining the coupling solution between the same mover

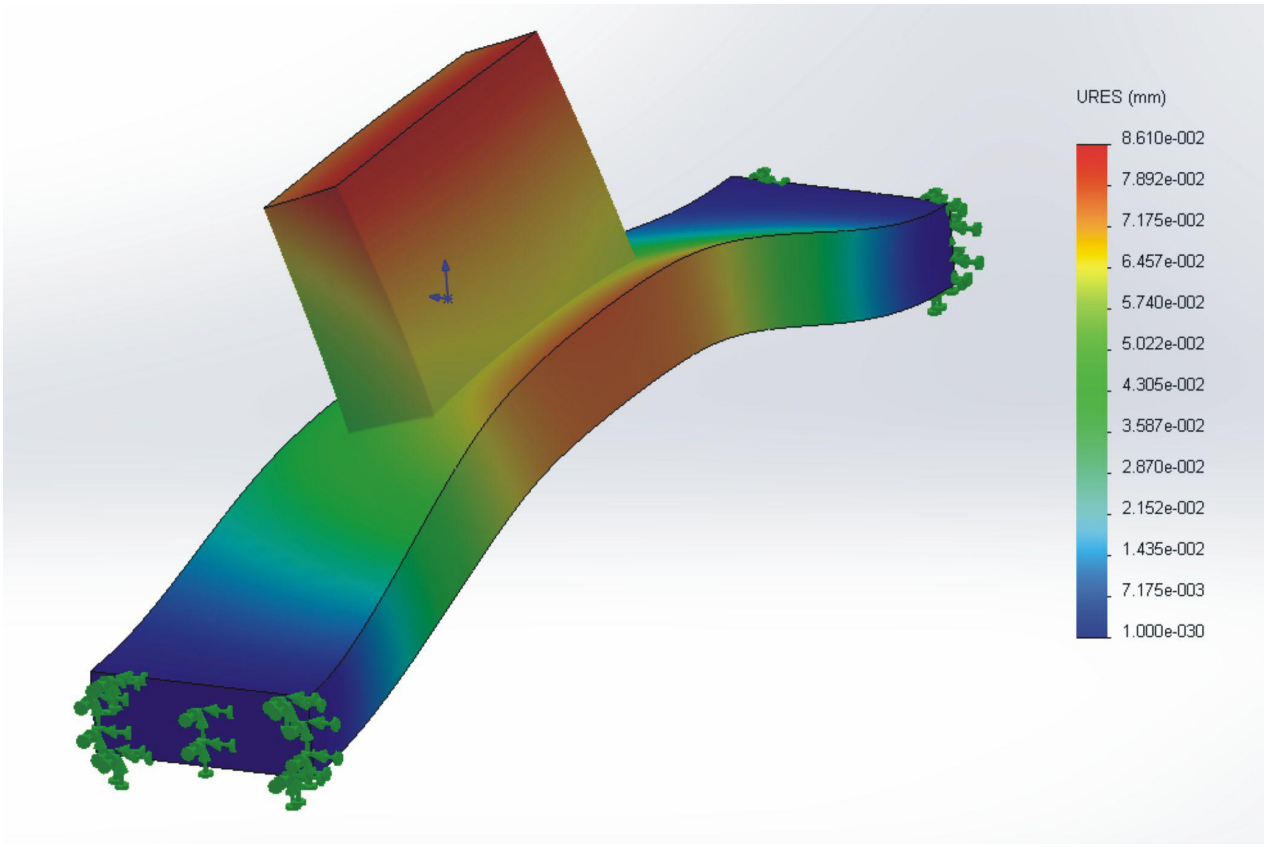

Figure 18: Deformed shape of the polar expansion and base enbloc.

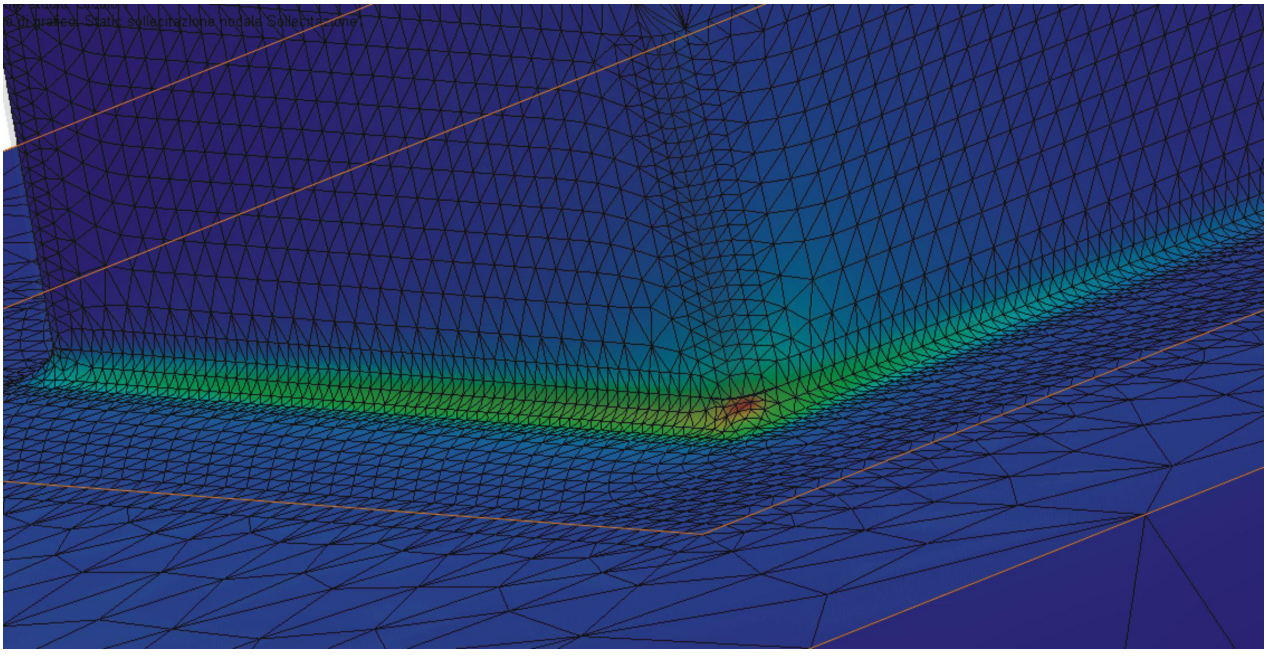

Figure 19: Stress concentration in the polar expansion and base enbloc.

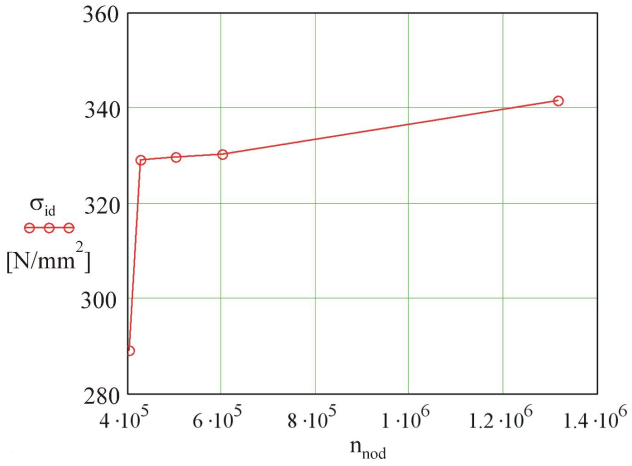

Figure 20: Convergence curve to check the stress σ_{id} in the area where the three edges of the pole piece intersect (see Figure 19, fillet radius R=0.5 mm).

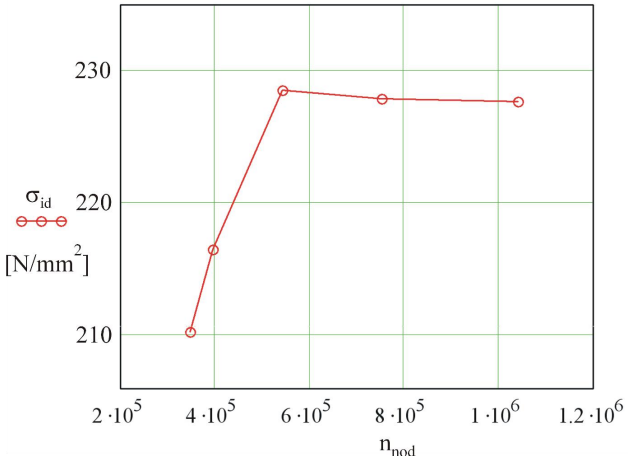

Figure 21: Convergence curve to check the stress σ_{id} in the area where the three edges of the pole piece intersect (see Figure 19, fillet radius R=1 mm).

Table 5: Order of Magnitude in the Engine Room.

Displacement	0.25 mm
Velocity	30 mm/s
Acceleration	20 mm/s^2
Frequency	5-300 Hz

and the structure of the frame. Others aspects that have to be considered for the design of larger actuators regard the deformations and vibrations of the hull in the zone where the actuator will be installed. In the following paragraphs these aspects will be carefully examined in order to correctly address the mechanical design of larger linear electromagnetic actuators.

Table 6: Ida Teresa Ship.

Gross tonnage	16000 ton
Length	177 m
Width	23 m
Height	14 m
Velocity	17 knots
Power	11500 CV
Propeller	125 rpm
Engine	Diesel

8.1 Causes of Possible Deformations of the Actuator

The deformations of the actuator can be due to i) failure to compliance with the dimensional and geometric tolerances [19–23] of the various components, ii) stresses induced by the electromagnetic forces generated by the device, iii) hull deformations, and iv) vibrations. In relation to the dimensional and geometric tolerances, we can note that the larger the dimensions of the parts that constitute the actuator are, the greater the difficult to satisfy such tolerances. The correct sliding of the mover in the correspondent slide guides is obtained by maintaining the air gap between the retention cages of the magnets and polar expansions as constant as possible. Furthermore, small air gap changes (for example less than 10%) during the movement of the mover can also meaningfully influence the thrust value and the forces applied to the slide guides. In such a case, an electronic control system of the thrust must be able to effectively operate. However, the guides on the side of the mover where the air gap is diminished are highly stressed and their life decrease. Concerning this aspect, for example, with reference to a nominal air gap equal to 3 mm, the maximum change of the air gap to minimize the negative effects previously mentioned should not be greater than 0.3 mm. In relation to the deformations induced by the electromagnetic forces generated by the device (see the forces applied to the polar expansions that have been considered to perform the FEM computations described in Section 5), in general it is always possible to define an adequate dimensioning of the system so as to reduce such deformations. With reference to the deformations of the hull we observe that the actuator is installed in the same hull by suitable joints. If the hull warps, such joints can strain the actuator by causing it to malfunction. In relation to this possible problem, it is convenient to distinguish the hull deformations due to vibrations and those caused by hydrodynamic actions. The order of magnitude of the vibrations in the en-

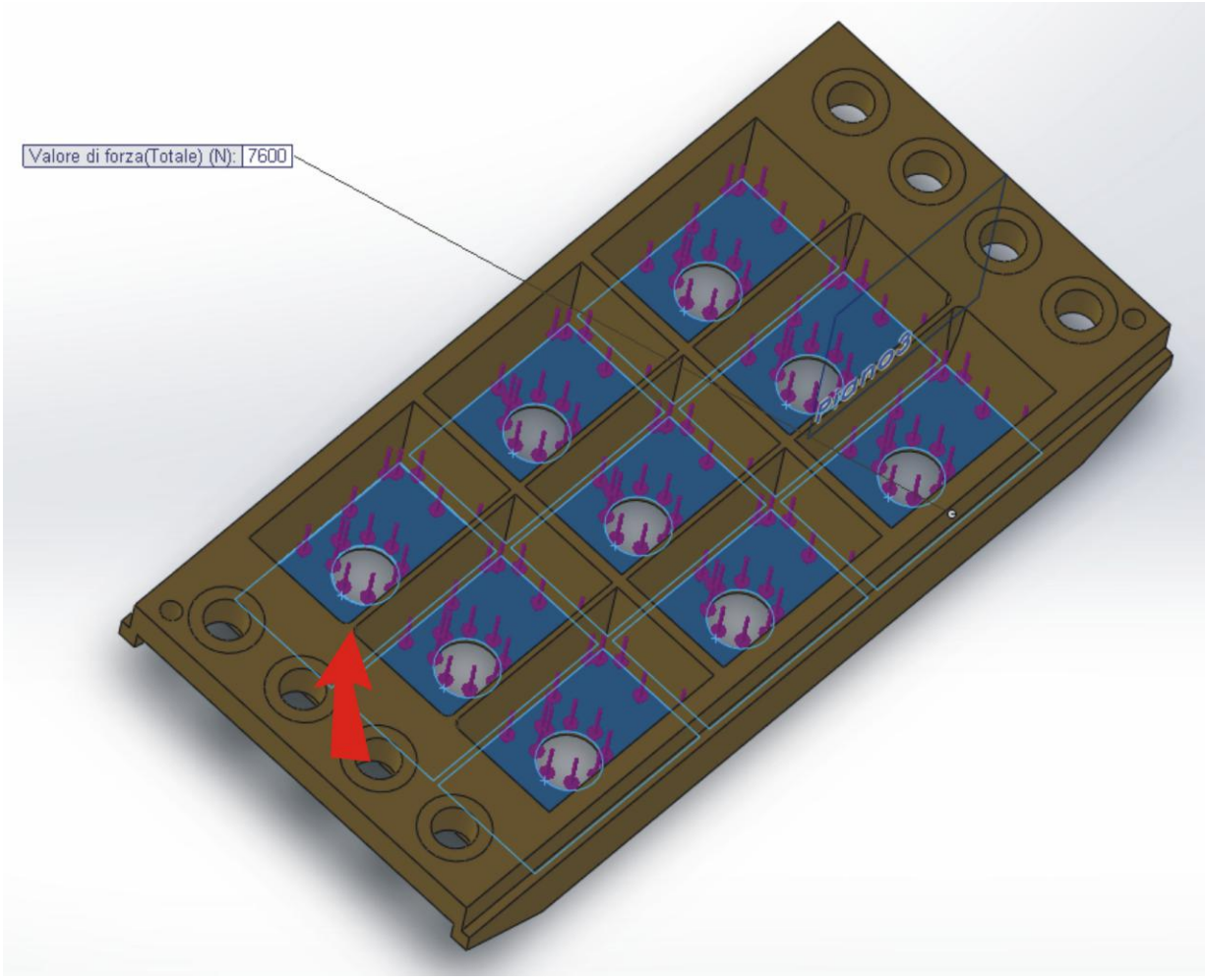

Figure 22: Forces perpendicular to the housing bottom surfaces of the magnets retention cage to perform FEM analyses.

gine room of ships is reported in Table 5. We note that acceptable displacements are equal up to 0.25 mm with frequencies between 5 and 300 Hz. These displacements in general are caused by local resonances due to excitation harmonics that are generated by the propellers and/or the engines. Other causes of the above-mentioned displacements can be the instability of the rudder (a driving system resonance of the rudder can take place). In relation to this aspect we can cite the case of the *Ida Teresa* ship (http://maritime-connector.com/ship/friday-6513982/) that was used for the transport of the grain. In Table 6 some characteristics of this cargo ship are reported. The *Ida Teresa* showed irregular vibrations, non linear, across the whole hull, often with very low frequencies (5 Hz) and remarkable amplitude. These vibrations affected in particular the stern zone: the problem consisted in a resonance between the hydraulic cylinders that drove the rudder and the system hull-rudder-control levers subject to the hydrodynamic forces. The problem was empirically resolved by a control system of the oil efflux through the hydraulic cylinders. This case represents an example of how problems can arise regarding rudder control systems of large vessels and the difficulty of predicting them by numerical simulations. Basically, too many parameters are very difficult to identify and/or ill-defined (for example: stiffness, interactions among levers, rudder, hydrodynamic actions, hull, etc.). Consequently, an actuator for driving the rudder, in unfortunate cases could present problems of the type described. One way to try to prevent these drawbacks surely consists in manufacturing driving solutions as stiff as possible, with minimum clearances, and resonance frequencies generally high, away from the frequencies of the excitation harmonics that arise from the interaction hull-propeller-rudder-levers. Moreover, we note that these frequencies are not very predictable, although they are generally high depending on the angular velocity of the propeller. However, from the control point of view, the electromagnetic linear actuator is definitely more controllable

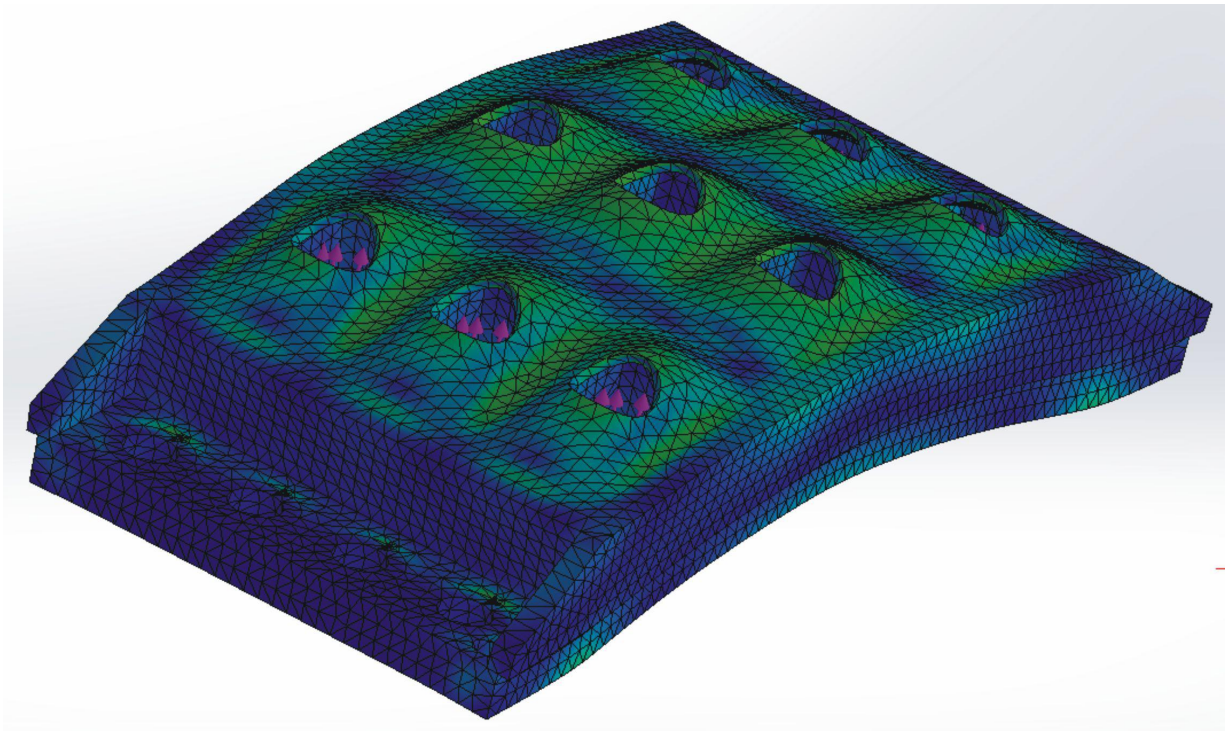

Figure 23: FEM simulation of the retention cage of the magnets.

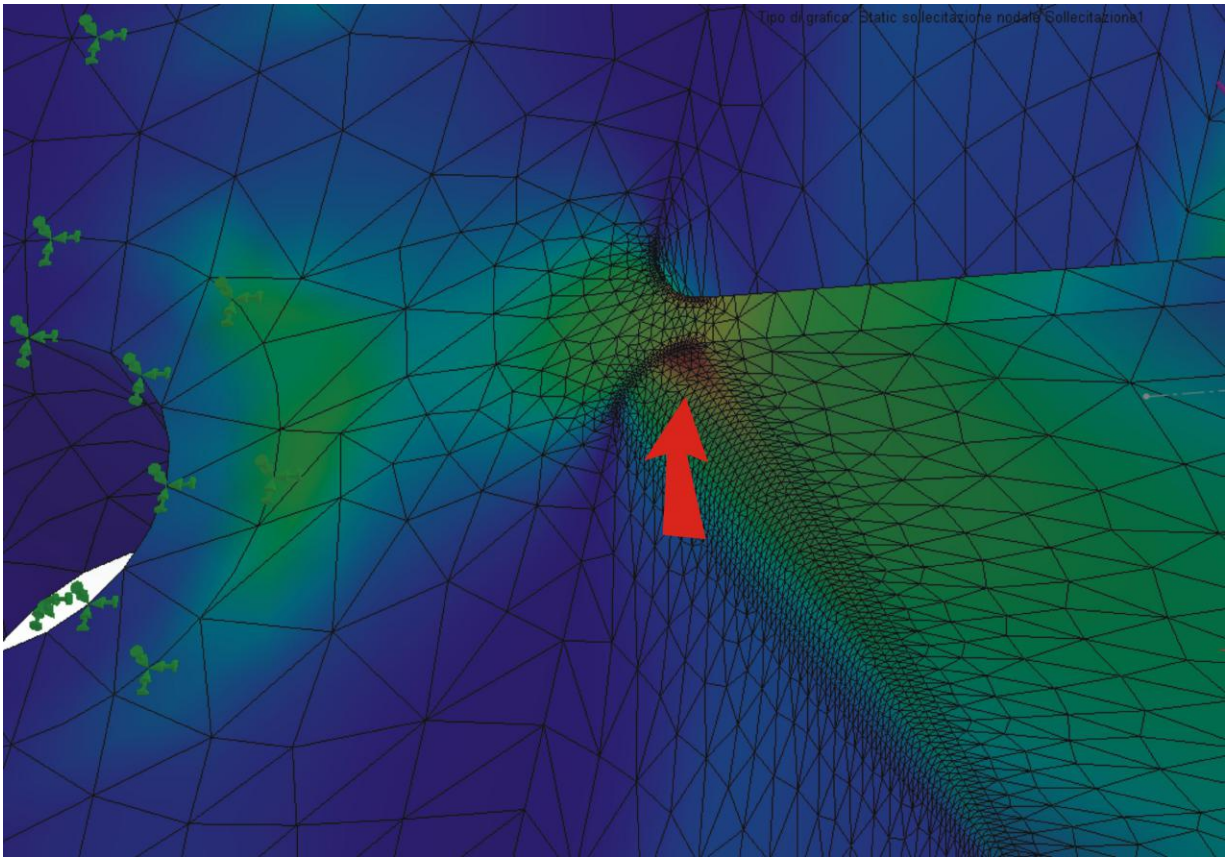

Figure 24: Stresses concentration on the filleted edge.

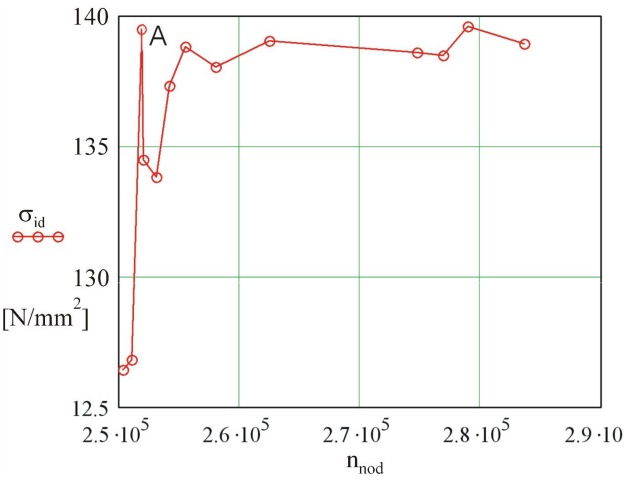

Figure 25: Convergence curve relative to the maximum stress σ_{id} indicated in Figure 24.

than a hydraulic one. Consequently, if problems similar to those previously described arise, the possibilities of intervention based on control of the voltage/current supply of the actuator can immediately adjust the thrust and reduce/eliminate harmful resonances. This kind of control would be more effective than the case in which hydraulic actuators are used. In relation to the hull deformation generally caused by the hydrodynamic actions during a normal navigation, unfortunately, experimental data are not available. However, some interior shootings that qualitatively illustrate the deformations of the between-decks of large ships during navigation with particularly rough sea are available. In these shootings a succession of watertight doors all the same type and dimension aligned along a between-deck in the longitudinal direction of the ship are shown: from the shootings the displacement between the first watertight door and the last one can be estimated). These deformations induced by the intense hydrodynamic actions applied to the hull, are apparent in correspondence to the cross sections of the same hull. For example, the deformation of bending/ torsion along the axis of such vessels determines high relative displacements between two cross sections about twenty meters away. As a matter of fact, the value of these displacements can be also equal to 50 mm. In the engine room, where actuators for driving the rudders can be installed, there are no data regarding the deformations of the hull. However, in relation to the installation of multi-cylinder engines in line of high dimension in the engine room of big ships it was found that the weight of these motors (hundreds of tons) can cause displacements less or equal than 5-10 mm between two hull cross-sections one about 12 m away from the other. This finding is particularly important in relation to the assembly of the engines of the ship. For example, some diesel engines 12 m long, 2.6 m width, and 4.8 m height are installed in the engine room on a rigid sub-base by using wedges placed between the base surface of the engine and the sub-base. The sub-base is suitably connected to the hull by damping suspensions and the motor is joined to the sub-base by screws. The wedges are made of resin and are inserted hot before connecting the motor to the sub-base: thus the still warm resin can deform and compensate the various errors of flatness, straightness, etc. [23] of the contact surfaces engine/sub-base and especially the deformations of the hull caused by the weight of the engine. The previous data gives an idea of the stiffness of the engine room structure and it can be inferred that it is more rigid than the other parts of the ship. Consequently, even if intense hydrodynamic actions are applied to the hull, we can think that in such areas of the ship high deformations as those of the upper decks will not occur. This fact is particularly important in relation to the installation of linear electromagnetic actuators in the stern area (usually near to the engine room). A linear electromagnetic actuator able to develop at least a thrust equal to 30 tons will certainly be longer than the one already manufactured and illustrated in Figure 27. For example, by considering a frame 2 m long (the frame of the prototype is about 1 m long, see Figure 10), the joint points of the frame actuator-hull will be more distant from one another. It was noted that the displacement of the points where the actuator will be fixed due to the causes previously discussed is not known. However, one can reasonably assume that the greater the distance between these points, the higher the probability that in a certain instant the relative displacement between these joint points is maximum. This fact can cause anomalous deformations of the actuator. Since these deformations are very important in relation to the reliable functioning of electromagnetic actuators of which the length is greater than 1 m, a qualitative in-depth analysis of this aspect is carried out in the following paragraph.

8.2 Qualitative Analysis for the Evaluation of the Actuator Stress/Strain

Figure 1 shows the area where a pair of oil-pressure rotary actuators [1, 7, 8] for driving the two rudders of a military vessel are installed. The solution considers the connection of the two actuators by the horizontal bar highlighted in the picture by the red arrow. The distance between the two actuators is equal to 4500 mm (see Figure 1). During normal operating conditions only one actuator drives both rudders: the other actuator remains con-

Figure 26: Forces perpendicular to the side surfaces of the retention cage housings to perform FEM analyses.

nected to the one running, but is not active. In this way, in case of malfunction concerning the active actuator, the other actuator can immediately come into operation because it is already mechanically connected to the system of levers which drives the pair of rudders. It is also noted that each of the two actuators is connected to the hull by means of two plates. Each plate is joined to the structure of the ship by four screws. In Figure 1 these screws are denoted by the numbers 1, 2, 3, and 4. The sections X-X and Y-Y are very close to the axes of the respective pairs of screws 1, 2 and 3, 4. Two of these screws are clearly visible in the photograph of the engine room that houses the hydraulic actuators (see the area highlighted by an ellipse in Figure 1). These two sections are virtually identical and overlap each other in Figure 28. The separate representation of these sections is shown in Figure 29. A possible qualitative torsional deformation of the hull in correspondence to the same sections is shown in Figure 30. It is noted that the magnitude of the deformation illustrated is actually very small because the sections X-X and Y-Y are very close. In Figure 31 the pairs of connection plates of each actuator are shown in detail and we observe that the distance between the two sections X-X and Y-Y is only equal to 830 mm. It follows that the deformation shown in Figure 30 is certainly very small under any navigation conditions. The width of the plates is also very small (350 mm), therefore even if the deformations of the hull are relatively high, the plates remain essentially flat. The horizontal distance from the center of gravity of each pair of plates is instead equal to 1.36 m (see Figure 31). It was seen that in general the greater this distance, the higher the probability that the two pairs of plates do not belong to the same horizontal plane. In this case a deformation would be imposed to all the parts that are connected to these plates, in particular to the structure of the actuators. With reference to the ship where the pair of oil-pressure rotary actuators is installed (a Maestrale class ship of the Italian Navy), no malfunctioning due to an excessive deformation of the hull transmitted by these plates to the actuators has been noticed. However, especially in navigation, certain time varying deformations affect the transverse section of the hull, in particular in correspondence to the sections X-X and Y-Y, even if they have never been measured. The magnitude of such deformation is surely lower than the longitudinal one. Moreover, since the hull cross section of the military ships in general is smaller than that of the commer-

Figure 27: The linear electromagnetic actuator manufactured and tested (the red arrow indicate the force sensor to measure the thurst furnished by the actuator).

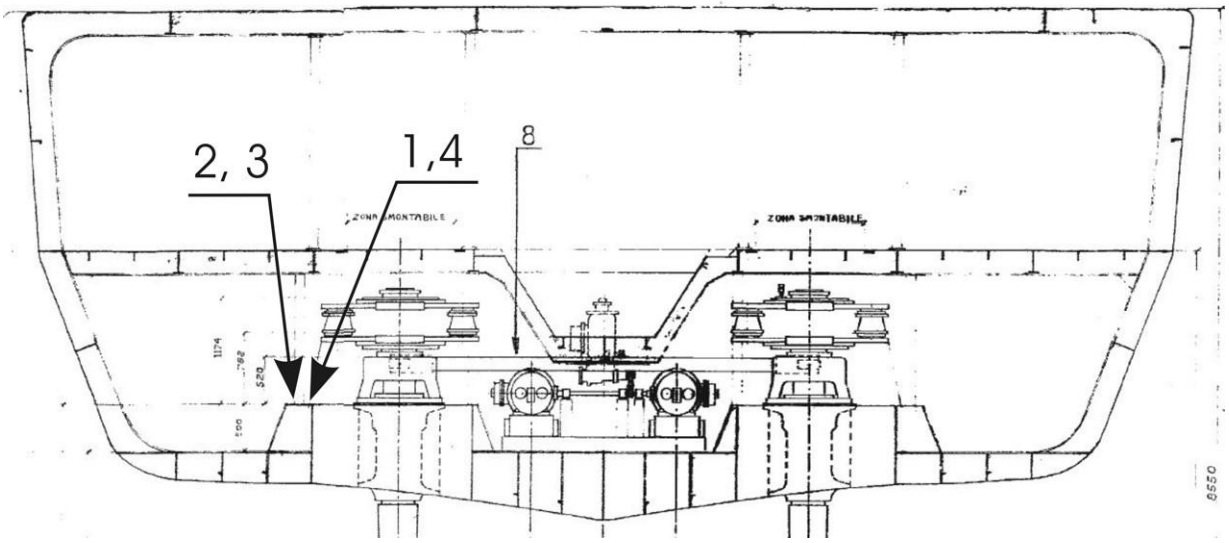

Figure 28: Overlapping of the hull cross sections X-X and Y-Y where the oil-pressure rotary actuators are installed.

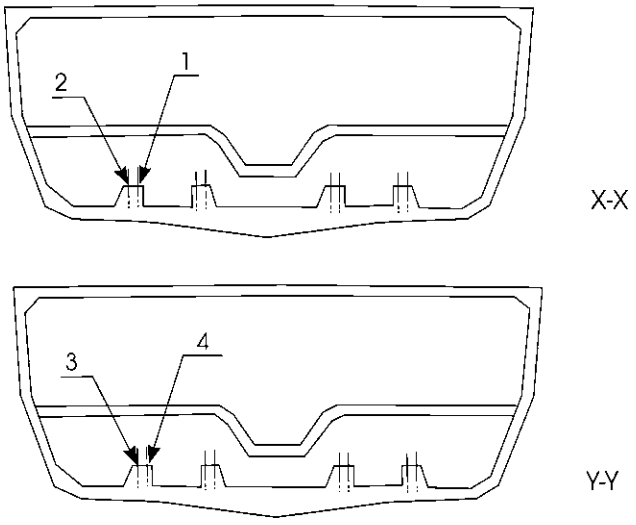

Figure 29: Separate cross sections X-X and Y-Y.

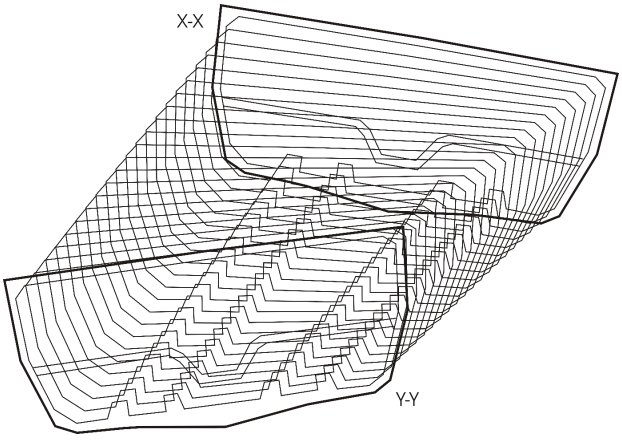

Figure 30: Hull deformation in the sections X-X and Y-Y (in correspondence to the screw joints of the oil-pressure rotary actuators brackets).

cial ones, the transverse deformations will be contained. Nevertheless, in the case of replacement of the hydraulic actuators with a linear electromagnetic actuator, it is necessary to pay particular attention to this aspect. The most logical choice would be to join the electromagnetic actuator by using the joint areas where the previous hydraulic actuator had been connected. Anyway, the geometry of the electromagnetic actuator is very different and above all, its length can be high. In relation to the higher length, the version of the actuator able to develop a thrust equal to 30 ton or more could have six connection brackets to the hull (the prototype illustrated in Figure 5 has only four brackets: in the case of a more powerful and longer actuator, in order to improve the connection to the hull, one can reasonably consider another pair of intermediate brackets between those pre-existing). Since the mechanical reliability of the electromagnetic actuator is highly dependent on the correct sliding of the mover along the guides, it is essential that the functioning clearances of the slide bearings are respected. In relation to this aspect, if the brackets are subjected to displacements due to deformations of the hull, there are two design choices to avoid excessive deformation of the actuator frame resulting in reduction/zeroing of the functioning clearances. They are i) to increase the stiffness of the actuator frame and/or ii) to consider a significantly soft connection of the brackets to the hull (*e.g.* by inserting between the contact surfaces of the brackets-

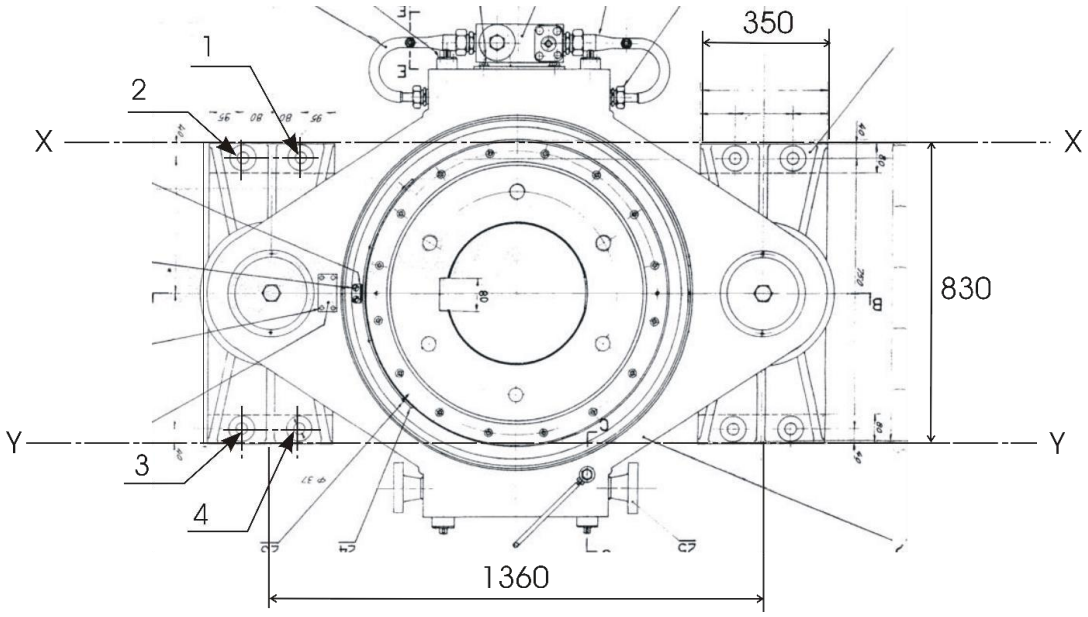

Figure 31: Dimensions of the joint plates between the oil-pressure rotary actuators and the hull.

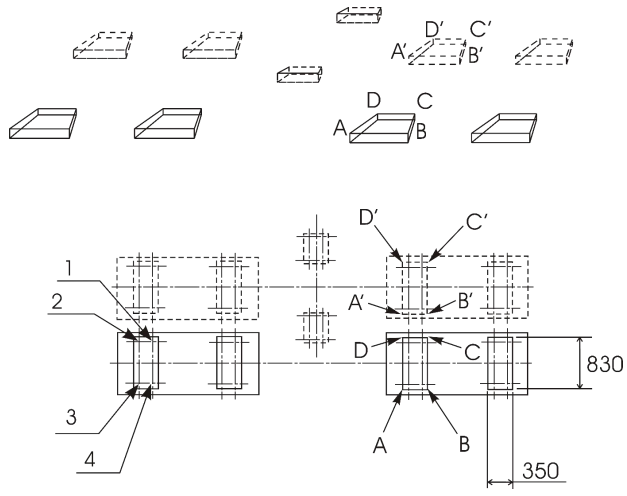

Figure 32: Possible positions of the rectangular plates where the brackets of a linear electromagnetic actuator could be fixed.

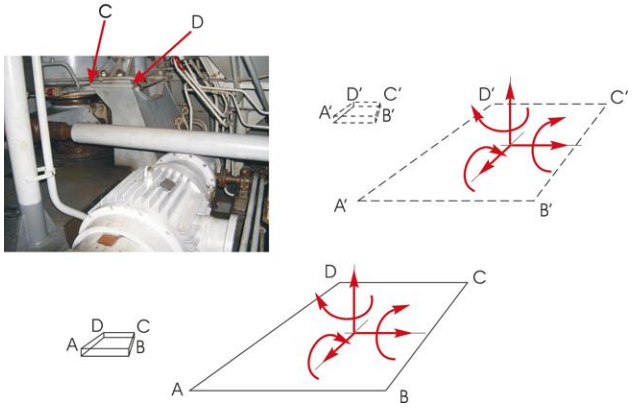

Figure 33: Rectilinear and rotational displacements applied to the joint brackets of the frame of the linear electromagnetic actuator.

hull a suitable elastomeric material able to take up the relative displacements in the areas of connection). However, the design of actuators greater than the prototype shown in Figure 27 must be validated by reliable structural calculations that allow a proper evaluation of the deformation of the actuator caused by the possible displacements imposed by the brackets. In relation to the complexity of the system geometry it will definitely be convenient to perform structural analysis by finite elements (FEM). Concerning this aspect, Figure 32 shows the vertices A, B, C, D and A', B', C', D' of the rectangular surfaces pair where the brackets of an oil-pressure rotary actuator are fixed. In correspondence of the centers of gravity of these surfaces, the degrees of freedom (DOF) of the surfaces considered as rigid bodies in the space have been indicated by the red arrows. The brackets fixed to the hull apply forces and displacements to the plates fixed to the actuator along the above-mentioned degrees of freedom (see Figure 33). Since the electromagnetic actuator must be fixed on similar surfaces, each of them will apply to the corresponding bracket stresses/displacements along similar degrees of freedom. Figure 34 illustrates the solid modeling of the electromagnetic actuator prototype already manufactured (see Figure 27) graphically modified (the actuator has only been slightly elongated to make it similar to what the 30 ton actuator might be). We note the forces/external mo-

ments or linear/angular displacements (indicated by the red arrows) that the brackets could apply to the actuator frame when relative displacements of the joint surfaces to the hull occur (see the DOF represented by the red arrows in the previous Figure 33). Therefore, in order to be sure that the functioning clearances of the slide guides are maintained, the design of large linear electromagnetic actuators should be definitely validated by structural computations based on finite element models of the actuator frame (stator) to which, as shown in Figure 34, appropriate forces/displacements are imposed. The value of these forces/displacements that have to be used in order to perform the numerical simulations should be obtained by experimental measurements executed within the hull of the ship during various conditions of navigation exactly in the areas where the brackets of the electromagnetic actuator will be fixed. In relation to the problem of assuring the functioning clearances of the guides, the following paragraph discusses a possible alternative to the recirculating ball bearings used in the prototype shown in Figure 27. This new solution should allow a proper adjustment of the clearances so as to ensure the functionality of actuators longer and wider than that has already been manufactured, even when sensible deformations of the same actuators frames occurs. With the proposed solution the clearances could easily adjust i) during the assembly of the device so as to compensate the various dimensional, flatness, parallelism, etc. errors [19–23] originated from the manufacturing and/or ii) during the tests of the device in the hull of the ship.

8.3 A Conceptual Solution for Long Linear Actuators

The prototype actuator (see Figure 27) used recirculating ball bearing guides. These guides allow the sliding of the mover through the stator. In Figures 5, 6, 35, and 36(a) the bearings and their positioning in the structure are illustrated. Since the maximum distance between the bearings did not exceed 1.0 m, no particular problem to obtain a precise relative positioning of these bearings has been noted. As a matter of fact, the normal manufacturing tolerances of the various parts and the precision of the structure assembly made it possible to get a good sliding of the mover in the guides. This result has been achieved because the frame had a small size and consequently the various errors of flatness, straightness, etc. of the surfaces of the side members on which the recirculating ball bearing had been fixed were small. Therefore, without particular adjustments of the positioning of these bearings, a good result has been obtained. However, the increase of the lengths of the side members surely causes greater geometrical errors and the alignment of the bearings can become

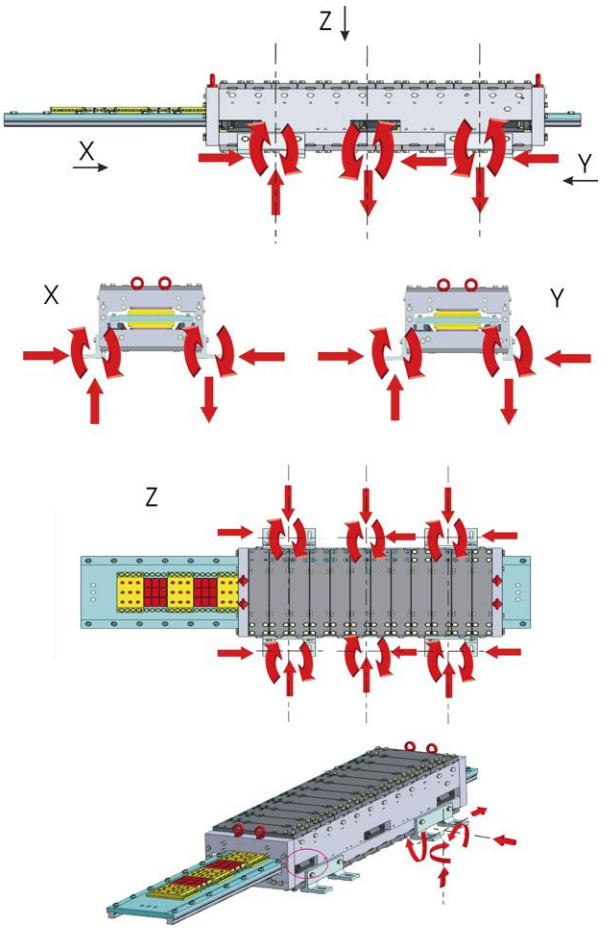

Figure 34: Forces and moments imposed to the actuator frame to the joint brackets.

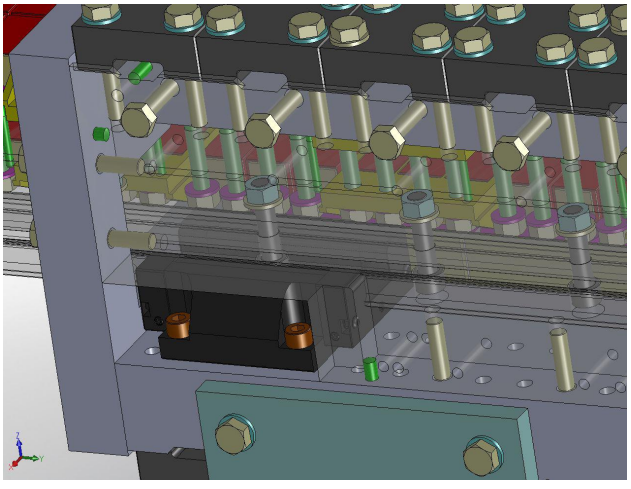

Figure 35: Recirculating ball bearings used in the electromagnetic actuator prototype.

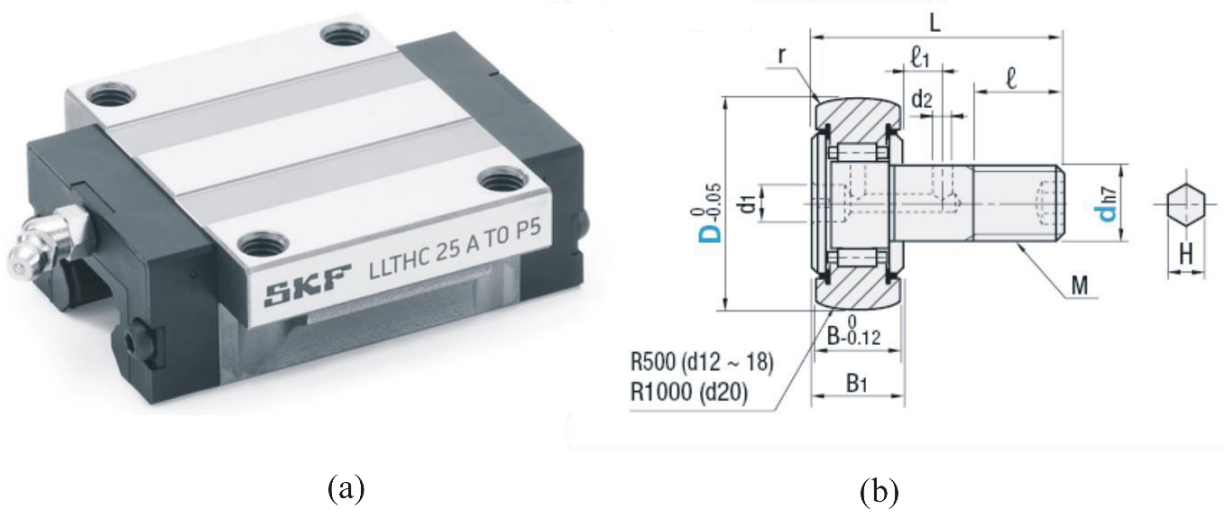

Figure 36: (a) Recirculating ball bearing and (b) cam follower bearing.

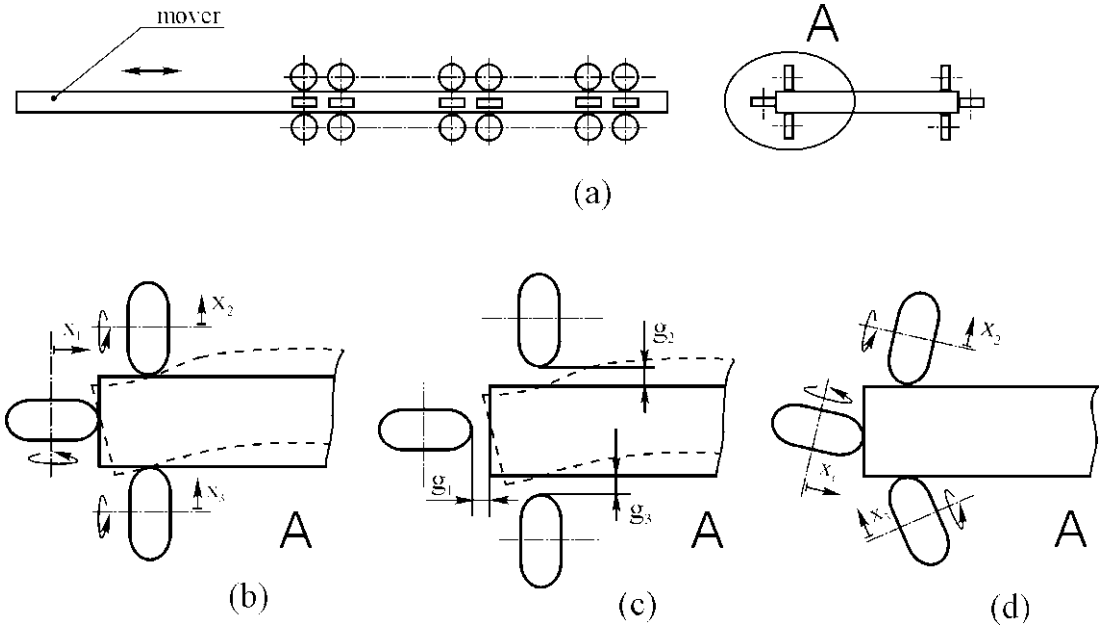

Figure 37: (a) Mover and cam follower bearings, (b) rectilinear degrees of freedom x_1, x_2, and x_3 of three cam follower bearings, (c) adjustable clearances g_1, g_2, and g_3, (d) perpendicularity errors of the cam follower bearings.

problematic. Assuming to manufacture a frame of the device approximately twice as long as the one already made, it is almost sure that by using the usual manufacturing tolerances, problems of coupling between the mover and the stator will arise. The functional clearances of the bearing could be resetted to zero and, depending on the mover position during its motion, forcings will occur. Therefore, the utilization of recirculating ball bearings of the type shown in Figure 36(a) simply assembled on the longerons of a frame 2 m long can be problematic. The solution to machine the seats of such bearings by smaller tolerances in order to ensure a good alignment of the bearings most distant each from one another, could be too expensive. Moreover, this choice would not allow an easy adjustment of the bearings alignments when the assembling of the system is finished. A conceptual design that can be considered to reduce/remove the drawbacks previously described is based on the use of cam followers with concentric seat. A section of this kind of bearing is illustrated in Figure 36(b). In these devices the external surface of the outer ring is toric. The inner ring is a pin with a usually threaded end in order to allow a stable fastening of the bearing. Figure 37(a) shows

the conceptual solution that, for example, considers the use of 36 cam followers. The outer ring of each bearing is nominally placed in contact with the corresponding flat surface of the mover of which the cross section has a rectangular shape. The bearing pins are joined to the frame of the actuator by a screw connection. This mechanical connection can be loosened or tightened so as to enable the adjustment of each bearing along a direction nominally perpendicular to the flat contact surface of the mover. The enlarged detail A (see Figure 37(b)) illustrates the three degrees of freedom x_1, x_2, and x_3 relative to three bearings of which the axes of rotation belong to the same plane. Therefore one can adjust with high precision the functioning clerances denoted by g_1, g_2, and g_3 (see Figure 36(c)). Since the surfaces of the outer rings of the bearings are toric, if the rectangular plate (*i.e.* the mover) should tilt and/or warp, a proper point contact between the bearings and the same mover will always be assured (see the mover profile dash line in Figure 37(b)). Moreover, even if the rotation axes of the bearings are not perfectly perpendicular to the contact flat surfaces of the mover, the toroidal shape of the outer ring will allow a correct sliding of the same mover (see Figure 37(d)). This situation could arise when there is a certain perpendicularity error [23] between the axis of the bearing pins and the flat side walls of the actuator frame on which the pins have to be fixed. Even in this case it will be possible to adjust the functioning clearances by g_1, g_2, and g_3 previously mentioned. Therefore, by this solution 36 adjustable functioning clearances g_1, g_2, …, g_{36} will be defined. The possibility of adjusting the clearances is particularly important because i) it enables one to properly compensate the machining errors of the frame in relation to those of the mover, ii) it is possible to precisely adjust the maximum and the minimum clearances and all the other 24 intermediate clearances in order to obtain a good sliding of the mover during the assembly phase in the workroom, iii) when the actuator is assembled inside the hull and/or when the navigation problems occur (*i.e.* forcing of the stator structure due to unforeseen deformations of the hull), we can try to eliminate/reduce a possible mover forcing by adjusting in situ one or more of the 36 clearances $g_1, g_2, \ldots, g_{36}$, iv) if during the dock/navigation tests, actuator vibration problems are noticed, we can try to eliminate/reduce them by appropriate adjustments of the above-mentioned clearances. As a matter of fact, concerning this last observation passing over the unfortunate cases (very difficult to predict) of the classical resonance problems that could be solved by changing the actuator stiffness/damping and/or the stator-hull joints, local vibrations in the actuator could arise. These vibrations are not due to the resonance, but can cause problems. The following paragraph discusses the nature of this kind of vibration with reference to mechanical systems very different from one another, but that can be associated with the same type of vibration. The paragraph finishes with an illustration of possible negative influences of these vibrations and possible design features to reduce the probability that they occur.

8.4 Possible Negative Effects of Local Vibrations

Some mechanical systems show local vibrations with small amplitude that are caused by external forces. These forces can often be driving moments/forces or other applied moments/forces that change periodically. One or more harmonics of these exciting causes can induce local vibrations of certain parts of the motion transmission system. These vibrations have generally nothing to do with the vibrations due to system resonances. Therefore, they are forced local vibrations. Some transmission systems of motion are often constituted by coupled parts that move each relatively to the others. Consequently, in order to enable a regular operation of the device, functioning clearances between each pair of coupled parts are defined. Therefore such parts have one or more degrees of freedom that enable the relative motion. The stiffness of these systems depend on the stiffness of i) each part, ii) the possible film of lubricant, and iii) other elements of which the stiffness is not easy to identify. In relation to the micro bumps between the above-mentioned parts (due to the functioning clearances), the mechanical system can locally be forced to vibrate at the frequency of one or more harmonic components of excitation that propagates through the whole system of motion transmission. However, it is not excluded that locally, these vibrating subsystems can be characterized by particularly damped resonance frequencies that can be excited by the harmonics previously mentioned. Since these vibrating subsystems can change their configuration during the motion depending on the same excitation forces, the vibrations that arise are often of non-linear kind, *i.e.* stiffness and/or damping depend on the position/velocity of the various parts versus time. The stiffnesses locally depend on the clearances and/or the other parameters above-mentioned, therefore it is sufficient that such parameters change very little (due to the wear, the lubricant thickness, the manufacturing dimensional and geometric tolerances, etc.) to cause or not to cause the occurrence of the vibrations previously cited. It follows that these vibrations are difficult to predict. As a matter of fact, even if nominally identical sys-

tems are considered, the vibrations could affect one system but not the other. For the same reason, it can be very difficult to identify the cause of such vibrations and their elimination can be problematic. These vibrations, in general do not cause the collapse of the system as would be the case in situations of "classical" resonance of the whole system. However, the type of "local" vibrations we have discussed can produce malfunctioning of the system by modyfing its correct functioning and/or reducing the service life. Moreover, expensive maintenance and frequent replacements of the components that have been damaged by the local vibrations could be necessary. This kind of vibrations could be classified as chaotic vibrations [24–27] which are deterministic, but from an analytical point of view, unpredictable. In some real cases the vibrations here defined as "local" and "chaotic" were found. Typical examples occurred in the bearings of the transmission shaft of towboats. The vibrations detected in correspondence with the bearings supports inexplicably exceeded the safe limits that assured the correct service life of the same bearings. The transmission system, also equipped with universal joints, was not subject to resonance at all, but the frequency of the excessive vibrations of the bearings corresponded to that of a harmonic of engine torque transmitted through the shaft transmission. However, another transmission system of another towboat nominally identical to that above discussed, did not show any particular vibrations (the vibrations of the bearings were within the limits). Other cases of anomalous vibrations affecting completely different systems from the towboats transmission shafts, have been reported with reference to plate rolling mills [28] and also in rotary presses. In these devices the anomalous vibrations have been indirectly detected owing to the negative effects on the product obtained during the machine operation. Concerning this aspect, in the case of the rolling-mill process of thin steel sheets for pressing bonnets and/or other parts of the car bodywork, it was noticed that the painted surface of the pressed sheet often showed faults. As a matter of fact, it was not possible to perfectly paint the surface of the sheet already pressed: some painted areas were affected by unexplained and unsightly reflections. Therefore, a thickness change of the rolled sheet was detected. This pseudo periodic and/or random thickness change was ascribed to the rolling process. During the rolling, the rolls of the plate mill have been subjected to a very small local vibration (the whole plate mill certainly did not vibrate unlike when torsional vibrations occur [29]: these kind of vibrations would produce macroscopic drawbacks). Conversely, the local vibrations had a very small magnitude, but had locally involved bearings and supports of one or more rolling cylinders, also in relation to the stiffness of the sheet that was rolled. Consequently, the distance between the rolls axes was not maintained strictly constant: this fact caused the variability of the thickness of the rolled product, undetectable to the naked eye, but visible with reflected light (after the painting). Similar problems of vibrations have been found in relation to the influence of the stiffness of the paper thickness during the print phase of newspapers by rotary presses. With reference to these cases we observe that the hull of a vessel is often subject to vibrations more or less intense, especially near the engine room. Excitations in general can be generated by the engines and the interaction of the system hull-water-propellers [30]. In certain particularly unfortunate and unpredictable cases, the vibrations transmitted from the hull to the electromagnetic actuator can cause local negative effects during its operation. Since the mover has to be able to slide within the structure of the stator as shown in Figure 37, the functioning clearances g_1, g_2, …, g_{36} definitely allow small displacements of the mover along the vertical direction. It follows that if the magnetic forces developed during various functioning conditions can not retain the mover in a stable position along the vertical direction, the above-mentioned vibrations can cause local collisions between the same mover and the cam follower bearings. Should this problem occur, the countermeasures to consider could be the following: i) utilization of selective damping joints to connect the actuator to the hull, ii) development of an electronic feedback control that can change the attractive forces exerted by the actuator polar expansions on the mover so as to always keep it in contact with the bearings of the upper or lower side and with the bearings of only one lateral side of the same mover, iii) to consider a mechanical system of adjustable elastic preloading to always ensure the contact of the mover with the bearings. For example, the dynamic behaviour of the above-mentioned preloading system could be based on analytical modelizations similar to those developed in [31, 32].

9 Conclusions

The transition from the conceptual design of a new kind of electromagnetic linear actuator (see Figure 2) into a working design (see Figures 4-8, 27) has been carried out by considering the following factors: i) decrease of all the maximum mechanical deformations (evaluated by the Finite Element Method) of the system to no more than 8/100 mm with respect to the unstrained configuration, ii) minimization of the overall dimensions, iii) assembly

and transport ease, iv) reliability of the mover translation mechanism, and v) elimination of the lateral instability danger of the mover during the development of the thrust. The solution found has allowed a compact, rigid and low cost device to be obtained. The choice among various kinds of base-pole piece joints of the machine has been made according to the results obtained by the FEM simulations and the easiness of manufacturing (especially in relation to the manufacturing cost). From the structural strength and deformation point of view, all the choices can be judged sufficiently reliable (at least with reference to the manufacturing of a first actuator prototype). Consequently, according to the cheapness criterion, it was decided to manufacture the system base-polar expansion enbloc (see Figures 8). With regard to the retention cages, in relation to the high strength aluminum alloy that has been chosen to manufacture them (see Table 1), the FEM analyses indicate that stresses and deformations are acceptable, even if the permanent magnets lose their magnetization. In accordance with the results of the structural analyses performed, the actuator has been manufactured and tested. The performances obtained were similar to those computed by the electromagnetic computations [11]. The 3D modeling and FEM simulations have been carried out by using SolidWorks and Simulation softwares [18], respectively. In relation to further developments of linear electromagnetic actuators of which the dimensions are greater than those of the prototype already manufactured (see Figure 27), this study performed an analysis of the problems that have to be considered to obtain a reliable design. In this regard, an ulterior change relating to the manufacturing of the ferromagnetic cores was taken into account. In the prototype actuator, the ferromagnetic cores were enbloc: thin, insulated iron sheets, lying, as much as possible, parallel with the lines of flux were not used. This cores enbloc choice has been possible because the current frequencies that supply the actuator are extremely low. Consequently, the losses that occur in the ferromagnetic core due to hysteresis and eddy currents are low. As a matter of fact these losses only cause a small heating. In this way, by adopting cores enbloc, an increase in the structural strength and stiffness of the actuator have been obtained. However, in anticipation of i) increasing the size of the system, ii) higher supply current, and iii) utilization of inverters with current frequencies greater than 2 Hz to get higher thrusts, the insulated iron sheets for manufacturing the ferromagnetic cores has to be reconsidered.

References

[1] Akers A., Gassman M., Smith R., Hydraulic Power System Analysis, CRC Press, Taylor and Francis, 2006

[2] Liu S., Chang X., Synchro-control of Twin-rudder with Cloud Model, International Journal of Automation and Computing, February 2012, 9, 1, 98-104

[3] Sari D. P., Design Control System Ship Stability Corvette SIGMA-366 Hassanudin Using Linear and Nonlinear With Water Wave Sea State 6, EPH, International Journal of Science and Engineering, November 2016, 2, Issue11, Paper-6

[4] Muscari R., Dubbioso G., Viviani M., Di Mascio A., Analysis of the asymmetric behavior of propeller–rudder system of twin screw ships by CFD, Ocean Engineering, In Press, Corrected Proof, Available online 31 July 2017

[5] Zhang Y., Li Y., Sun Y., Zeng J., Wan L., Design and simulation of X-rudder AUV's motion control, Ocean Engineering, 2017, 137, 204–214

[6] Tessarolo A., Internal Report on the Electromagnetic Linear Actuator Prototype – Project ISO (Innovative Solutions for Italian Navy's Onboard Full-Electric Actuators), University of Trieste, 2013

[7] Bruzzese C., Santini E., Tessarolo A., Menis R., Sidoti D., Development of new electric direct-drives for replacement of oleodynamic actuators on board military ships–Electric Direct-Drive Actuator (EDDA), PNRM research project joint proposal, University of Rome – Sapienza and University of Trieste, 2013

[8] Bruzzese, C., A high absolute thrust permanent magnet linear actuator for direct drive of ship's steering gears: Concept and FEM analysis, In: Proceedings of ICEM Conference (Sept. 2-5, 2012, Marseille, France), 2012

[9] Tessarolo A., Bruzzese C., Computationally-Efficient Thermal Analysis of a Low-Speed High-Thrust Linear Electric Actuator with a 3D Thernal Network Approach, IEEE Transactions on Industrial Electronics, 2015, http://ieeexplore.ieee.org/stamp/stamp.jsp?tp=&arnumber=6861986&isnumber=4387790

[10] Tessarolo A., Bruzzese C., Mazzuca T., Scala G., A novel fault-tolerant high-thrust inverter-controlled permanent magnet linear actuator for direct-drive of shipboard loads, In: IEEE (Ed.), Proceedings of the IEEE Electric Ship Technology Symposium, IEEE ESTS 2013 (22-24 April 2013, Arlington, VA, USA), IEEE, 2013, 459-463

[11] Bruzzese C., Tessarolo A., Mazucca T., G. Scala, A High-Thrust Linear Electric Motor Prototype for Perspective Replacement of Shipboard Hydraulic Actuators, In: Proceedings of AEIT'13 International Conference (3-5 October, 2013, Palermo, Italy), 2013

[12] Bortolozzi M., Bruzzese C., Ferro F., Mazzuca T., Mezzarobba M., Scala G., Tessarolo A., Zito D., Magnetic Optimization of a Fault-Tolerant Linear Permanent Magnet Modular Actuator for Shipboard Applications, In: IEEE (Ed.), Proceedings of SDEMPED 2013 (27-30 Aug 2013, Valencia, Spain), IEEE, 2013

[13] Mazzucca T., Bruzzese C., Project ISO: Innovative Solutions for Italian Navy's Onboard Full-Electric Actuators, In: IEEE (Ed.), Proceedings of IEEE ESARS 2012 (16-18 October, 2012, Bologna, Italy), 2012

[14] Melosh R. J., Finite element analysis convergence curves, Finite Elements in Analysis and Design, November 1982, vol. 7, Issue 2, 115-121

[15] Melosh R. J., Identifying the characteristics of finite elemet analysis convergences curves, Finite Elements in Analysis and Design, June 1993, vol. 13, Issue 2-3, 105-113
[16] Veyhl C., Belova I. V., Murch G. E., Öchsner A., Fiedler T., On the mesh dependence of non-linear mechanical finite element analysis, Finite Elements in Analysis and Design, June 2010, 46, pp. 371-378
[17] Prathap G., Naganarayana B. P., Stress oscillations and spurious load mechanisms in variationally inconsistent assumed strain formulations, International Journal for Numerical Methods in Engineering, 1992, vol. 33, 2181-2197
[18] SolidWorks, Dassault Systems SolidWorks Corporation, http://www.solidworks.com
[19] UNI EN ISO 14405-1:2011, Geometrical product specifications (GPS) - Dimensional tolerancing - Part 1: Linear sizes
[20] UNI EN ISO 286-2:2010, Geometrical product specifications (GPS) - ISO code system for tolerances on linear sizes - Part 2: Tables of standard tolerance classes and limit deviations for holes and shafts
[21] UNI EN ISO 286-1:2010, Geometrical product specifications (GPS) - ISO code system for tolerances on linear sizes - Part 1: Basis of tolerances, deviations and fits
[22] UNI ISO/TR 16570:2007, Geometrical product specifications (GPS) - Linear and angular dimensioning and tolerancing: +/– limit specifications - Step dimensions, distances, angular sizes and radii
[23] UNI EN ISO 1101:2013, Geometrical product specifications (GPS) - Geometrical tolerancing - Tolerances of form, orientation, location and run-out
[24] Gu P., Dubowsky S., The Design Implications of Chaotic and Near-Chaotic Vibrations in Machines, In: Proceedings of ASME Design Engineering Technical Conference (13-16 September 1998, Atlanta, GA, USA)
[25] Gu P., Dubowsky S., Chaotic Vibration and Design Criteria for Machine Systems with Clearance Connections, In: Proceedings of the Ninth World Congress of the Theory Machines and Mechanism (1-3 September 1995, Milan, Italy)
[26] Awrejcwicz J., Krysko A. V., Yakovleva T. V., Zelenchuk D. S., Krysko V.A., Chaotic Synchronization of Vibrations of a Coupled Mechanical System Consisting of a Plate and Beams, Latin American Journal of Solid and Structures, 2013, 10, 163-174
[27] Sado D., Kot M., Chaotic Vibration of an Autoparametrical System with a Non Ideal Source of Power, Journal of Theoretical and Applied Mechanics, 2007, 45, 119-131
[28] Freites R., Fernández E., Merlino H., Rodríguez D., Britos P., García-Martínez R., Frictional Defects in Cold Rolling of Tin Plate Diagnostic, In: IEEE (Ed.), Proceedings of CERMA 2007 Electronics, Robotics & Automotive Mechanics Conference (25-28 September 2007, Cuernavaca, Morelos, Mexico.), IEEE, 2007, 303-306
[29] Han D., Shi P., Xia K., Non linear Torsional Dynamics Behaviuor of Rolling Mill's Multi-DOF Main Drive System under Parametric Excitation, Journal of Applied Mathematics, Article ID 202686, 2014
[30] Barrass C.B., Ship Design and Performance for Masters and Mates, Chapter 20, Ship Vibration, 191-201, Elsevier Editor, 2004
[31] Stanescu N. D, Popa D., Stability of the Equilibrium Positions of an Engine with Nonlinear Quadratic Springs, Central European Journal of Engineering, 2014, 4, Issue 2, 170-177
[32] Harris C. M., Piersol A. G., Harris'Shock and Vibration Handbook, Chapter 3, 5th ed., Mc Graw Hill, 2002